

1 Dear Dr. Harman,

2

3

4

5

6 We would like to thank you and both the anonymous reviewers for those comments and  
7 suggestions which helped to improve the paper. As per your suggestion of minor revision  
8 before publication, we have included the model calibration and validation from the other  
9 paper into this paper. By doing this we avoid citation of the other paper, which has been  
10 rejected. We have also responded to the comments that were given by reviewer #2 and  
11 acknowledged the limitations of the study that are related to the shift in Plant Functional  
12 Types (PFTs) due to climate change (increase in temperature) and the impact on vegetation of  
13 increasing atmospheric CO<sub>2</sub>. We made these changes in the revised manuscript in which all  
14 changes are tracked in blue color.

15

16

17 Kind Regards,

18 Dr Yongping Wei

19

20

21

22

23

24

25

26

27

## 28 Authors' responses

29 Authors' responses (in blue) to Anonymous Referee #2 comments (in black) on "Including  
30 the dynamic relationship between climate variables and vegetation LAI into a hydrological  
31 model to improve streamflow prediction under climate change" by Z. K. Tesemma et al.

32

33 This study aims to predict future water yields incorporating vegetation dynamics in a VIC  
34 hydrological model based on two emission scenarios. This study is based on the assumption  
35 that seasonal vegetation dynamics strongly depend on accumulative water deficits  
36 (precipitation - potential evapotranspiration), developed for three plant functional types  
37 (PFTs) from global remote sensing datasets (MODIS). The paper starts with the critiques of  
38 stationarity assumption in future hydrological simulations. I totally agree to this point in that  
39 traditional hydrologic modeling has often ignored the importance of vegetation response to  
40 changing climates. However, the authors make a same mistake when applying Eq. 5 for the  
41 prediction of vegetation dynamics in the future. There are two main reasons why I reject this  
42 paper.

43 First, distributions of plant functional types would not be constant under climate changes.  
44 Each PFT shares similar ecophysiological behavior in photosynthesis and evapotranspiration,  
45 which is one of the reason why this study develops the different equations of vegetation  
46 dynamics for three PFTs. Therefore, the changes in PFT distributions are quite critical to  
47 predict ecosystem water use and resulting hydrologic behavior under climate change. The  
48 shifts of vegetation distributions in response to temperature increases and subsequent water  
49 balance are well-documented in Mediterranean climate regions (e.g. Lenihan et al. 2003;  
50 Crimmins et al. 2011), which significantly undermines the credibility of this study.

51 We understand the concern of Referee #2 on changes in plant functional types (PFTs) due to  
52 change in climate (increase in temperature) and in the revised version of the manuscript we  
53 acknowledged the limitation of our study in which static PFTs were used.

54 Here we would like to explain the rationale for why static PFTs were used in our study.  
55 Firstly, it is known that vegetation growth in Australia is highly controlled by precipitation  
56 (water supply), and is less controlled by temperature and radiation (Nemani et al., 2003).  
57 Hence, most vegetation dynamics can be explained by variation in precipitation, which  
58 formed the basis of the LAI-climate model developed in Tesemma et al. (2014). In our study

59 area PFTs are largely determined by land use (human activities), such as forest clearing for  
60 agriculture, which is difficult to project into the future, rather than natural responses of  
61 vegetation to changed climatic conditions. We agree with the reviewer that in theory there are  
62 possible changes in PFTs due to increased temperature, but in this catchment human  
63 influence are likely to dominate.

64 Second, the strong dependency of vegetation dynamics on water balance does not  
65 marginalize the CO<sub>2</sub> fertilization effect on vegetation. Many studies suggest that the CO<sub>2</sub>  
66 fertilization would decrease stomatal conductance, increase water use efficiency and drought  
67 tolerance (e.g. Nowak 2004; Ainsworth and Rogers 2007). While this CO<sub>2</sub> effect can be  
68 limited by nutrient supply in temperate forests (e.g. Oren et al. 2001), water-limited  
69 ecosystems would be benefited from increased water use efficiency (Wullschleger et al.  
70 2002; Huang et al 2007; Koutavas et al. 2012). Therefore, many ecologists suggest that an  
71 interaction with CO<sub>2</sub> should not be ignored, when we model vegetation responses to droughts  
72 in the future.

73 Several ecohydrologists have tried to deconvolve the effect of precipitation, temperature and  
74 CO<sub>2</sub> in the future hydrological modeling across different ecoregions (e.g. Baron et al. 2000).  
75 Tague et al. (2009) suggested that future hydrologic behavior and ecosystem productivity will  
76 depend on the balance between CO<sub>2</sub> controls on water use efficiency and vegetation  
77 responses to climate changes in Mediterranean climate region. Vicente-Serrano et al. (2015)  
78 suggested that the effect of rising CO<sub>2</sub> on canopy-level productivity might be strongly  
79 mediated by moisture conditions from mesic to xeric sites in temperate conifer forests.  
80 Interactions between vegetation and hydrology can be particularly important in the water-  
81 limited ecosystems, where vegetation dynamics and its water use are strongly coupled, as  
82 well as subsequent hydrologic behavior. However, few studies have considered the potential  
83 feedbacks between vegetation, climate, and hydrology in future hydrological modeling. I  
84 hope that hydrologists can start on the common ground with ecologists when including  
85 vegetation dynamics in future hydrological modeling under a changing climate.

86 Partially Agree. We understand the reviewers concern about the vegetation effect of  
87 increasing atmospheric CO<sub>2</sub> and we have already discussed this effect in the manuscript. We  
88 have modified our discussion of this issue slightly to clarify our assumption of not modelling  
89 this effect. The reason why we did not include the stomata suppression effects of rising  
90 atmospheric CO<sub>2</sub> is because the net impact on runoff could be small (Huntington, 2008;

91 Uddling et al., 2008) due to the offsetting nature of the fertilization effect on LAI. We believe  
92 the revised discussion deals with this issue sufficiently.

93

94

95 **References**

96 Huntington, T. G.: CO<sub>2</sub>-induced suppression of transpiration cannot explain increasing  
97 runoff, *Hydrol. Processes*, 2008.

98 Nemani, R. R., C. D. Keeling, H. Hashimoto, W. M. Jolly, S. C. Piper, C. J. Tucker, R. B.  
99 Myneni, and S. W. Running (2003), Climate-Driven Increases in Global Terrestrial Net  
100 Primary Production from 1982 to 1999, edited, p. 1560, American Association for the  
101 Advancement of Science.

102 Uddling, J., Teclaw, R. M., Kubiske, M. E., Pregitzer, K. S., and Ellsworth, D. S.: Sap flux in  
103 pure aspen and mixed aspen–birch forests exposed to elevated concentrations of carbon  
104 dioxide and ozone, *Tree Physiol.*, 28, 1231-1243, 2008.

105 Tesemma, Z. K., Y. Wei, A. W. Western, and M. C. Peel (2014), Leaf Area Index Variation  
106 for Crop, Pasture, and Tree in Response to Climatic Variation in the Goulburn–Broken  
107 Catchment, Australia, *Journal of Hydrometeorology*, 15(4), 1592-1606.

108

109

110

111

112

113

114

115

116

117

118 **Including the dynamic relationship between climate variables and**  
119 **leaf area index in a hydrological model to improve streamflow**  
120 **prediction under a changing climate**

121

122 **Z. K. Tesemma<sup>1</sup>; Y. Wei<sup>1</sup>; M. C. Peel<sup>1</sup> and A. W. Western<sup>1</sup>**

123 [1] Department of Infrastructure Engineering, The University of Melbourne, Parkville,  
124 Victoria, 3010, Australia.

125 Correspondence to: Yongping Wei ([ywei@unimelb.edu.au](mailto:ywei@unimelb.edu.au))

126

127 **Abstract**

128 Anthropogenic climate change is projected to enrich the atmosphere with carbon dioxide,  
129 change vegetation dynamics and influence the availability of water at the catchment [scale](#).  
130 This study combines a non-linear model for estimating changes in leaf area index (LAI) due  
131 to climate fluctuations with the Variable Infiltration Capacity (VIC) hydrological model to  
132 improve catchment streamflow prediction under a changing climate. The combined model  
133 was applied to thirteen gauged catchments with different land cover types (crop, pasture and  
134 tree) in the Goulburn-Broken Catchment, Australia for the “Millennium Drought” (1997–  
135 2009) relative to the period (1983–1995), and for two future periods (2021–2050 and 2071–  
136 2100) for two emission scenarios (RCP4.5 and RCP8.5) were compared with the baseline  
137 historical period of 1981–2010. This region was projected to be warmer and mostly drier in  
138 the future as predicted by 38 Coupled Model Inter-comparison Project Phase 5 (CMIP5) runs  
139 from 15 Global Climate Models (GCMs) and for two emission scenarios. The results showed  
140 that during the Millennium Drought there was about a 29.7%–66.3% reduction in mean  
141 annual runoff due to reduced precipitation and increased temperature. When drought induced  
142 changes in LAI are included, smaller reductions in mean annual runoff of between 29.3% and  
143 61.4% were predicted. The proportional increase in runoff due to modelling LAI was 1.3%–  
144 10.2% relative to not including LAI. For projected climate change under the RCP4.5  
145 emission scenario ignoring the LAI response to changing climate could lead to a further  
146 reduction in mean annual runoff of between 2.3% and 27.7% in the near-term (2021–2050)  
147 and 2.3% to 23.1% later in the century (2071–2100) relative to modelling the dynamic  
148 response of LAI to precipitation and temperature changes. Similar results (near-term 2.5% to

149 25.9% and end of century 2.6% to 24.2%) were found for climate change under the RCP8.5  
150 emission scenario. Incorporating climate-induced changes in LAI in [the](#) VIC model reduced  
151 the projected declines in streamflow and confirms the importance of including the effects of  
152 changes in LAI in future projections of streamflow.

153

154 Key words: Climate change, leaf area index, drought, catchment streamflow, vegetation  
155 dynamics, VIC hydrological model.

## 156 **1 Introduction**

157 Recently, climate changes have been observed in different parts of Australia (Chiew et al.,  
158 2011; Cai and Cowan, 2008; Hughes et al., 2012; Lockart et al., 2009; Potter and Chiew,  
159 2011). Specifically, south-eastern Australian catchments have experienced changes in  
160 streamflow due to fluctuations in climate as observed during the recent “Millennium  
161 Drought” (1997-2009) which lasted more than a decade (Chiew et al., 2011; Verdon-Kidd  
162 and Kiem, 2009). This drought may be representative of future climatic conditions in this  
163 region.

164 The projected water availability for future climates derived from downscaled outputs from  
165 global and regional climate models indicate increases of mean annual runoff by 10% to 40%  
166 in some parts of the world (high northern latitudes) and 10% to 30% reduction elsewhere  
167 (southern Europe, Middle East and south-eastern Australia) (Milly et al., 2005). More  
168 recently, Roderick and Farquhar (2011) examined climate and catchment characteristics for  
169 sensitivity to changes in runoff in Murray-Darling Basin in southeast Australia from a  
170 theoretical point of view and estimated that a 10% change in precipitation would lead to a  
171 26% change in runoff and a 10% change in potential evaporation would lead to a 16% change  
172 in runoff with all other variables being constant. In south-eastern Australia it has been  
173 projected that there will be a reduction in mean annual runoff of 10% on average when  
174 different climate models are used as input to hydrological models (Cai and Cowan, 2008;  
175 Chiew et al., 2009; Roderick and Farquhar, 2011; Teng et al., 2012a; Vaze and Teng, 2011).  
176 These studies assessed the possible impacts of climate change on total runoff based on  
177 rainfall-runoff relationships which only considered first order effects of changes in  
178 precipitation and temperature with subsequent impacts on evaporative demand.

179 There is evidence that such relationships are not stationary over time (Chiew et al., 2014;  
180 Peel and Blöschl, 2011; Vaze et al., 2010), which implies that the studies discussed in the  
181 previous paragraph may be missing an important factor. One approach to improving  
182 modelling under changing conditions is to use variable monthly leaf area index (LAI) in the  
183 hydrologic model. Using observed climate variability and streamflow responses, observed  
184 monthly LAI has been shown to improve [soil moisture prediction \(Ford and Quiring, 2013\)](#).  
185 The improvements are largest under either relatively wet or dry climatic conditions, i.e. in  
186 wet and dry years, rather than average years. In most south-eastern Australia, LAI primarily  
187 responds to the availability of water and changes in vegetation type, such as conversion of  
188 forest to cropland or pasture, but also responds, to a lesser extent, to changes in temperature

189 and rising atmospheric CO<sub>2</sub> concentrations. Most of these LAI responses are expected to be  
190 affected by projected climate change. These climate-induced changes in vegetation LAI may  
191 impact on evapotranspiration and runoff and hence should be considered when making runoff  
192 projections for climate change scenarios.

193 Dynamic Global Vegetation Models (DGVMs) have been used to assess the vegetation effect  
194 of climate change on large-scale hydrological processes and patterns (Murray et al., 2012a,  
195 2011). A list of available DGVMs and their processes representations (photosynthesis,  
196 respiration, allocation, and phenology) can be found in Wullschleger et al. (2014), while  
197 Scheiter et al. (2013) provides a review of the possible sources of uncertainty related to  
198 representation of plant functional type (PFT) in DGVMs. Most DGVMs overestimate runoff;  
199 mainly due to model structure problems along with operating at low spatial and temporal  
200 resolution (Murray et al., 2012b). While the relationships between LAI and climate  
201 fluctuation have been modelled (Ellis and Hatton, 2008; O'Grady et al., 2011; Jahan and Gan,  
202 2011; Palmer et al., 2010; Tesemma et al., 2014; White et al., 2010), none of them have been  
203 incorporated in hydrological models for the purpose assessing future climate change impacts  
204 on streamflow. The poor hydrological sub models in DGVMs and the static vegetation in  
205 most hydrological models mean that importance of the indirect vegetation-related (LAI)  
206 effects relative to the direct effects of changes in precipitation and temperature on  
207 hydrological response at catchment scale have rarely been studied. This limits understanding  
208 of the linkages between climate fluctuations and vegetation dynamics, and their combined  
209 impacts on hydrological processes.

210 The main objective of this study is to examine the relative effects on mean annual runoff of  
211 changes in direct climate forcing (mainly precipitation and temperature) and direct climate  
212 forcing combined with climate-induced LAI changes under changed climate scenarios.  
213 Comparative analysis of these two cases enables the effect on mean annual runoff of allowing  
214 LAI to respond to a changing climate to be identified. Specifically, our study combined the  
215 LAI–Climate model developed in Tesemma et al. (2014) with the Variable Infiltration  
216 Capacity (VIC) hydrologic model to assess the impact on catchment runoff of how LAI is  
217 modelled (constant seasonal LAI or LAI varying in response to climate) under changing  
218 climatic conditions. As noted above, this combined model showed significant improvements  
219 in runoff simulations under historic conditions. Here we investigate two sets of changing  
220 climatic conditions: (1) the observed Millennium Drought (1997–2009), which is a persistent  
221 (>10 year) large change in climate; and (2) projected climate change for both wet and dry



222 catchments using 38 Coupled Model Inter-comparison Project Phase 5 (CMIP5) runs from 15  
223 different Global Climate Models (GCMs) for two future periods, 2021–2050 and 2071–2100,  
224 for two emission scenarios, RCP4.5 and RCP8.5). The results obtained from this study are  
225 expected to demonstrate whether modelling LAI in a way that responds to changing climatic  
226 conditions is important for modelling runoff during projected climate change in the study  
227 area.

## 228 **2 Research approach**

229 This section provides details about the dataset, the characteristics of the selected catchments  
230 and the modelling exercises. The catchment characteristics and dataset used in this study are  
231 briefly described in section 2.1. The application of multiple GCMs and emission scenarios  
232 output method are explained in section 2.2. The relationship between LAI and climatic  
233 variables are presented in section 2.3, and the hydrologic modelling experiment approach  
234 used to assess the impact of changes in climate on runoff are described in section 2.4.

### 235 **2.1 Catchment characteristics and dataset**

236 All the study catchments are located in the Goulburn-Broken Catchment which is a tributary  
237 of the Murray-Darling Basin, Australia. The Goulburn-Broken Catchment extends between  
238 35.8° to 37.7° S and between 144.6° to 146.7° E (Figure 1a) with a range of altitude from  
239 approximately 1790 m on the southern side to 86 m above mean sea level on the northern  
240 side of the catchment. The mean annual precipitation of the study catchments ranges from  
241 659 (in the north) to 1407 mm year<sup>-1</sup> (in the south) calculated for the period (1982–2012).  
242 The majority of the precipitation (about 60%) occurs during winter and spring. The reference  
243 potential evapotranspiration (PET) calculated using the Food and Agricultural Organization  
244 (FAO56) method, ranges from 903 mm year<sup>-1</sup> (in the north) to 1046 mm year<sup>-1</sup> (in the south).  
245 Hence, the dryness index (mean annual reference potential evapotranspiration divided by  
246 mean annual precipitation) varies from 0.64 to 1.6 (Figure 1b). The dominant land cover type  
247 in most of the catchments is forest (mainly tall open Eucalyptus forest and Eucalyptus  
248 woodlands) with some pasture in all catchments. A small amount of cropland is located in  
249 some of the catchments (Figure 1c).

250 Gridded input data used for the hydrological modelling include the daily precipitation,  
251 maximum and minimum temperature, vapour pressure and solar exposure data obtained from  
252 the Australian Water Availability Project (AWAP) of the Bureau of Meteorology (Jones et  
253 al., 2009) and gridded daily wind run data from McVicar et al. (2008) that was generated  
254 from point measurements. All data have a spatial resolution of 0.05° × 0.05° (approximately  
255 5km × 5km), and the period from 1982 to 2012 was selected for this study. The daily  
256 streamflow data at the outlet of the selected calibration catchments were obtained from the  
257 Victorian Water Resources Warehouse (<http://data.water.vic.gov.au/monitoring.htm>). The  
258 missed streamflow data were filled by regressing between neighbouring catchments. The  
259 elevation data were collected from the GEODATA 9 Second Digital Elevation Model (DEM-

260 9S) Version 3 (Geoscience Australia, 2008). The elevation data were resampled to a  
261 resolution of  $0.05^\circ \times 0.05^\circ$  using the spatial average. The land cover input data were derived  
262 from the National Dynamic Land Cover Dataset which provides a land cover map for the  
263 whole of Australia at a resolution of  $0.00235^\circ \times 0.00235^\circ$  (approximately 250m  $\times$  250m) and  
264 can be accessed at ([http://www.ga.gov.au/metadata-gateway/metadata/record/gcat\\_71071](http://www.ga.gov.au/metadata-gateway/metadata/record/gcat_71071)).  
265 LAI data were collected from the Global Land Surface Satellite (GLASS) product which is  
266 available for download from Beijing Normal University (<http://www.bnu-datacenter.com>).  
267 The soil parameters in the VIC model running resolution were derived from the five minute  
268 resolution Food and Agriculture Organization dataset (FAO, 1995). The root distribution in  
269 three soil layers was derived from the global ecosystem root distribution dataset (Schenk and  
270 Jackson, 2002).

## 271 **2.2 Applying multiple GCMs and multiple emission scenarios**

272 Outputs from many climate models from the Coupled Model Inter-comparison Project Phase  
273 5 (CMIP5) (Taylor et al., 2012) are used as input to the hydrological model. CMIP5 contains  
274 model runs for four representative concentration pathways (RCPs), which provide radiative  
275 forcing scenarios over the 21<sup>st</sup> century (Moss et al., 2010; Vuuren et al., 2011). In this study  
276 two emission scenarios were chosen: a midrange mitigation scenario, referred to as RCP4.5  
277 and a high emissions scenario RCP8.5 (Meinshausen et al., 2011). RCP4.5 results in a  
278 radiative forcing value of  $4.5 \text{ Wm}^{-2}$  at the end of the 21<sup>st</sup> century relative to the preindustrial  
279 value, while RCP8.5 provides a radiative forcing increase throughout the 21<sup>st</sup> century to a  
280 maximum of  $8.5 \text{ Wm}^{-2}$  at the end of the century.

281 CMIP5 Global Climate Model (GCM) data were obtained from (<http://climexp.knmi.nl>  
282 accessed 28 February 2014). These data were re-sampled to a common grid resolution of  $2.5^\circ$   
283 since each GCM has a different spatial resolution (some are the same, but most are different).  
284 A total of 38 RCP4.5 and RCP8.5 runs from 15 different GCM models have been used in this  
285 study to include the possible uncertainty among climate models. For each of the 38 runs,  
286 daily precipitation, minimum and maximum temperature data were collected for three  
287 periods, 1981–2010 (historical run), 2021–2050 and 2071–2100 (future runs). An assessment  
288 of the ability of the CMIP5 runs to reproduce the observed base line seasonality of  
289 precipitation, minimum and maximum temperature is shown in Figure 2. The seasonality in  
290 precipitation and temperature were well captured by most CMIP5 runs with biases which  
291 require correction.

292 Low spatial resolution GCM outputs require downscaling for application in catchment  
 293 hydrology studies. Here the ‘delta-change’ statistical downscaling technique was used to  
 294 downscale and bias-correct the GCM outputs (Fowler et al., 2007). Delta-change was  
 295 selected due to its low computational intensiveness and easy applicability to a range of  
 296 GCMs. We acknowledge the limitations of this method include an assumption of stationarity  
 297 in change factors, climate feedbacks are not incorporated and an inability to capture changes  
 298 in extreme events and year to year variability. Dynamic downscaling, which solves some of  
 299 these problems, was not used as it has high computational demand and is not readily available  
 300 for a range of GCM runs and scenarios (Fowler et al., 2007). A simple statistical downscaling  
 301 method was appropriate for this study as we were interested in the impact of including  
 302 climate induced LAI change on the runoff results. In the study area, the monthly LAI is  
 303 strongly related to three month and/or nine month moving average moisture state  
 304 (precipitation minus reference potential evapotranspiration) (Tesemma et al., 2014).  
 305 Therefore, so long as the precipitation is consistent between the two runs we can assess the  
 306 importance of the change in LAI representation between model runs. It has been suggested  
 307 that extreme precipitation might change differently to mean precipitation under climate  
 308 change (Harrold et al., 2005) and the delta-change method does not capture this. Nevertheless  
 309 delta-change was used as this study concentrates on average runoff which is strongly linked  
 310 to overall catchment wetness, rather than floods which are linked to a combination of  
 311 catchment wetness and extreme precipitation. Hence consideration of extreme precipitation  
 312 events is less important in this study.

313 Statistical downscaling was applied to each of the GCM outputs and emission scenarios.  
 314 Since the study area is covered by four GCM grid cells, the area weighted average  
 315 precipitation, minimum and maximum temperatures of the GCM grid cells covering the study  
 316 area were computed. The area weighted average values were then statistically downscaled  
 317 using the delta change approach. Delta changes were calculated separately for each of the 12  
 318 months. For temperatures the delta changes were calculated using

$$\Delta_T(j) = \bar{T}_{projn}(j) - \bar{T}_{baseline}(j) \quad (1)$$

319 where  $\Delta_T(j)$  is the delta change in the 30-year mean monthly minimum or maximum  
 320 temperature as simulated by the climate model for the future period and RCP of interest  
 321 (2021–2050 or 2071–2100, RCP4.5 or RCP8.5),  $\bar{T}_{projn}(j)$ , relative to the mean for the  
 322 baseline period (1981–2010) climate model simulation,  $\bar{T}_{baseline}(j)$ .  $j$  represents the month.

323  $\Delta_T(j)$  is then applied to the daily baseline (1980–2010) observations,  $T_{obs}(j,i)$ , for each pixel of  
 324 the climate gridded data (which is the same as the VIC model grid pixels) to obtain the  
 325 statistically downscaled minimum or maximum daily temperature,  $T_{\Delta}(j,i)$  for month  $j$  and  
 326 day  $i$ .

$$T_{\Delta}(j,i) = T_{obs}(j,i) + \Delta_T(j) \quad (2)$$

327 For precipitation, the delta changes value is computed as a proportional change rather than a  
 328 shift:

$$\Delta_p(j) = \frac{\bar{P}_{projn}(j)}{\bar{P}_{baseline}(j)} \quad (3)$$

329 and then applied to the observations using:

$$P_{\Delta}(j,i) = P_{obs}(j,i) \times \Delta_p(j) \quad (4)$$

330 Here  $\Delta_p(j)$  is the delta change in 30-year mean monthly precipitation as simulated by the  
 331 climate model  $\bar{P}_{projn}(j)$  for two future periods (2021–2050 and 2071–2100) relative to the  
 332 baseline simulation  $\bar{P}_{baseline}(j)$ ;  $P_{\Delta}(j,i)$  is the statistically downscaled daily precipitation for  
 333 the projected future climate change scenario for month  $j$  and day  $i$ ,  $P_{obs}(j,i)$  is observed daily  
 334 precipitation for the historical period (1981–2010) for month  $j$  and day  $i$  for each of the  
 335 precipitation pixel of the gridded climate data. The delta change approach maintains a similar  
 336 (but shifted or scaled) spatial variation of temperature and precipitation as that in the  
 337 historical observed gridded data. The daily pattern of weather variation and the relationships  
 338 between the various weather variables are also maintained. Because historic weather data  
 339 provides the basis for the temporal patterns, the well-recognized issue of “GCM drizzle” is  
 340 eliminated. The delta change method also corrects for differences between the mean elevation  
 341 of the four GCM grid cells by scaling up or down the historical spatial variation of  
 342 temperature and precipitation across the catchment.

### 343 **2.3 Relationship between LAI and climate variables**

344 Tesemma et al. (2014) showed that monthly LAI of each vegetation type was closely related  
 345 to changes in moisture state (precipitation minus reference evapotranspiration) of six-monthly  
 346 moving averages for crop and pasture, and nine-monthly moving averages for trees.  
 347 Differences in LAI response for the same change in moisture state among the three vegetation  
 348 types were also observed as differences in model parameters of the LAI–Climate relationship.  
 349 Tesemma et al. (2014) provides details on the derivation of the LAI–Climate relationship for

350 the Goulburn-Broken Catchment. The three LAI models developed for crop, pasture and tree  
 351 are given below.

$$352 \quad \text{LAI} = \begin{cases} \frac{136.4836}{1 + \exp\left(-\left(\frac{(P - \text{PET}) - 159.4555}{42.5607}\right)\right)}, & \text{if Crop} \\ \frac{6.2495}{1 + \exp\left(-\left(\frac{(P - \text{PET}) - 43.6157}{62.8487}\right)\right)}, & \text{if Pasture} \\ \frac{4.2091}{1 + \exp\left(-\left(\frac{(P - \text{PET}) + 57.1849}{36.9481}\right)\right)}, & \text{if Tree} \end{cases} \quad (5)$$

353 Where LAI is the leaf area index of the cover type (tree/pasture/crop), P is the six month  
 354 moving average of precipitation for crop and pasture, and the nine month moving average for  
 355 trees, and PET is the respective reference evapotranspiration.

356 The monthly LAI was then simulated for both historical and future climate scenarios using  
 357 the LAI–Climate model (Eq. 5) driven with the appropriate climate inputs. In this study  
 358 monthly average reference potential evapotranspiration (PET, mm day<sup>-1</sup>) was estimated using  
 359 the standard FAO Penman-Monteith daily computations (Allen et al., 1998) and then  
 360 aggregating to monthly values. The reference potential evapotranspiration for future climate  
 361 scenarios was computed using the projected minimum and maximum temperatures, while  
 362 incoming shortwave radiation and vapour pressure were derived from daily temperature  
 363 range using the algorithms of Kimball et al. (1997) and Thornton and Running (1999). The  
 364 wind speed was kept the same as the historical observations. A significant literature exists  
 365 (see discussion in Supplementary Material of McMahon et al., 2015) around the issue of  
 366 using temperature to drive future changes in reference potential evapotranspiration (PET).  
 367 We acknowledge this assumption and note that it is likely to have limited impact on our  
 368 runoff results in the mainly water limited catchments modelled here. The historical or future  
 369 precipitation was used in Eq. 5 according to the scenario being modelled. Potential LAI  
 370 variations in the baseline years (1981–2010) and the two future periods (2021–2050 and  
 371 2071–2100), for each of the two future emission scenarios, were simulated using the  
 372 downscaled outputs from the 38 CMIP5 runs of the 15 GCMs, as input into the LAI–Climate  
 373 model (Eq.5). The uncertainty ranges in modelled LAI that come from the difference in  
 374 climate input were determined by using the downscaled 38 CMIP5 runs individually in Eq. 5.

## 375 **2.4 Hydrological model and experimental design**

376 In this study we used the three layers VIC model (version 4.1.2g) to simulate streamflow. The  
377 VIC macroscale model is a spatially distributed conceptual hydrological model that balances  
378 both water and energy budgets over a grid cell. It simulates soil moisture, evapotranspiration,  
379 snow pack, runoff, baseflow and other hydrologic properties at daily or sub-daily time steps  
380 by solving both the governing water and energy balance equations (Liang et al., 1996). VIC  
381 estimates infiltration and runoff using the variable infiltration curve that represents the sub-  
382 grid spatial variability in soil moisture capacity (Liang et al., 1994; Zhao et al., 1995) and  
383 Penman-Monteith for potential evapotranspiration computation. The ability of the model to  
384 incorporate spatial representation of climate and inputs of soil, vegetation and other  
385 landscape properties make it applicable for climate and land use / land cover change impact  
386 studies. The VIC model has been widely used for a number of hydrological studies in  
387 different climatic zones across the globe (Zhao et al., 2012a; Zhao et al., 2012b; Cuo et al.,  
388 2013).

389 The seven most sensitive model parameters (b, Ds, Ws, Dsmax, d2, d3 and exp) in the VIC  
390 model (Demaria et al., 2007) were calibrated against observed streamflow from thirteen  
391 selected sub-catchments with different climate and land cover composition that are  
392 representative of the main runoff generating regions of the Goulburn-Broken catchment. The  
393 model parameters were calibrated separately for each selected unregulated sub-catchment and  
394 applied uniformly within a sub-catchment (Figure 1). The Multi-Objective Complex  
395 Evolution (MOCOM-UA) algorithm (Yapo et al., 1998) was used to calibrate the model. This  
396 algorithm was implemented on each of the selected catchments separately to calibrate the  
397 model against the observed runoff. The model was first calibrated for the entire period  
398 (1982–2012), then using the calibrated parameters as initial guesses, the model was re-  
399 calibrated for the period 1982–1997 and evaluated for the period 1998–2012. During the  
400 calibration, VIC ran on a daily basis but the objective function was calculated on a monthly  
401 basis. Three criteria (objective functions) were used to evaluate the model's performance  
402 during calibration: the Nash–Sutcliffe efficiency (NSE) (Nash and Sutcliffe, 1970) between  
403 observed and simulated flow, the logarithm of Nash–Sutcliffe efficiency (logNSE) which  
404 penalizes errors at peak flow, and the percentage bias from the observed mean flow (PBIAS).

405 VIC model was run at daily time step and input data with a 5km by 5km spatial grid  
406 resolution for 30 years from January 1981 to December 2010 to produce the baseline and  
407 experiment runs. Two model experiments were run: the first experiment considered the recent

408 historical climate (Millennium Drought, 1997–2009) and LAI estimates using the simple  
 409 LAI-Climate model against the relatively normal historical climate period (1983–1995). The  
 410 second experiment considered the future climate from 38 CMIP5 runs and corresponding LAI  
 411 derivatives for two periods (2021–2050 and 2071–2100), and two emission scenarios RCP4.5  
 412 and RCP8.5 with respect to the historical period (1981–2010). Both sets of simulations were  
 413 performed over the thirteen calibrated study catchments within the Goulburn-Broken  
 414 Catchment (Figure 1b). A flow chart of the modelling method is given in (Figure 3).

415 To identify the effect on mean annual runoff of allowing LAI to respond to a changing  
 416 climate, compared with LAI not responding, we used the following steps: (1) the calibrated  
 417 model was forced with inputs of historical climate data and LAI data modelled from using the  
 418 historical climate data (1981–2010) to establish baseline streamflow estimates; (2) the model  
 419 was forced with projected future climate inputs and corresponding modelled LAI to produce  
 420 projected streamflow for future scenarios; (3) the future climates were input along with the  
 421 LAI data used in step 1 to produce projected streamflow that ignore project LAI changes .  
 422 The difference in mean annual runoff between steps 3 and 1 represents the climate effect (*CC*  
 423 effect); on mean annual runoff of only Precipitation and Temperature. Whereas the difference  
 424 in mean annual runoff between steps 2 and 1 represents the net effect (*CC + LAI* effect); on  
 425 mean annual runoff of allowing LAI to respond to a changing climate in addition to the direct  
 426 climate forcing (Precipitation and Temperature). The difference in mean annual runoff  
 427 between steps 2 and 3 represents the component of the runoff response related to climate-  
 428 induced changes in LAI. For the millennium drought (1997–2009) the above two changes in  
 429 mean annual runoff were estimated in a similar fashion taking (1983–1995) time period as  
 430 relatively normal period. The percentage change of mean annual runoff against the historical  
 431 mean annual runoff for climate change effect ( $Q_{clim}$ ) (Eq. 6), climate change and LAI effect  
 432 ( $Q_{net}$ ) (Eq. 7); and the percentage of CC effect offset by LAI effect ( $Q_{lai}$ ) (Eq. 8) were  
 433 estimated as follows:

$$434 \quad Q_{clim} = \left[ \frac{100 * (Q_{historical LAI}^{future climate} - Q_{historical LAI}^{historical climate})}{Q_{historical LAI}^{historical climate}} \right] \quad (6)$$

$$435 \quad Q_{net} = \left[ \frac{100 * (Q_{future LAI}^{future climate} - Q_{historical LAI}^{historical climate})}{Q_{historical LAI}^{historical climate}} \right] \quad (7)$$

$$436 \quad Q_{lai} = \left[ \frac{100 * (Q_{clim} - Q_{net})}{Q_{net}} \right] \quad (8)$$



### 437 **3 Results**

438 This section provides results from the modelling exercises. [First the model calibration and](#)  
439 [evaluation are discussed in section 3.1.](#) The change in climate variables during: (1) the recent  
440 observed prolonged drought; and (2) future climate change projections for the study  
441 catchments are presented in section 3.2. The impact on both LAI (section 3.3) and catchment  
442 streamflow (section 3.4) of changes in climate input during the Millennium Drought and  
443 future climate change projections are also provided. These results provide readers with a  
444 comparison of the anticipated future change in climate with the recently observed drought.

#### 445 **3.1 Model calibration and evaluation results**

446 The calibrated model parameters and model performance during calibration (1982–1997) and  
447 evaluation (1998–2012) periods for each sub-catchment are listed in Table 1. Most of the  
448 calibrated catchments have NSE of more than 70% during both calibration and evaluation  
449 periods (Table 1). In most of the selected catchments the simulated runoff for both calibration  
450 and evaluation periods met the “satisfactory” criteria according to (Moriasi et al., 2007), with  
451  $NSE > 50\%$  and the percentage absolute bias is generally less than 25% during calibration  
452 and evaluation periods. Although VIC captured the temporal variability of runoff well, there  
453 were some systematic biases in the runoff simulated. The model overestimates peak flow in a  
454 few cases and underestimates low flow in most of the catchments. The sources of these biases  
455 need to be investigated in order to understand the performance of the model. To do this, the  
456 estimated monthly biases are plotted against the monthly climate inputs: precipitation,  
457 temperature and LAI (not shown here). The calibrated catchments showed no relationship  
458 between AWAP gridded climate data and simulated runoff biases. The biases are likely  
459 related to the model structure (Kalma et al., 1995) rather than the model inputs.

#### 460 **3.2 Change in the climate variables from change in climate**

##### 461 **3.2.1 Millennium drought**

462 The Millennium Drought brought a decline in the mean annual precipitation over the selected  
463 catchments which ranged from 17.9% to 24.1%, with a mean of 20.9% when compared with  
464 the period (1983–1995). It also brought an increase in mean annual temperature which ranged  
465 from 0.2° C to 0.4° C, with an average of 0.3° C as compared to the temperature in the period  
466 (1983–1995). All thirteen study catchments experienced a similar change in both  
467 precipitation and temperature (Table 2).

### 468 **3.2.2 Future climate**

469 Averaged over all 38 CMIP5 runs, the mean annual precipitation in 2021–2050 over the  
470 selected catchments is projected to decline by 2.9% and 3.7%, relative to the historical period  
471 1981–2010, under the RCP4.5 and RCP8.5 scenarios respectively. By the end of the century  
472 (2071–2100) mean annual precipitation is projected to decline by 5% and 5.2% under the  
473 RCP4.5 and RCP8.5 scenarios respectively (Table 3). The mean annual temperature is also  
474 projected to increase in both future periods and emission scenarios (Table 3).

475 Most precipitation projections showed a shift towards drier climates in all seasons except  
476 summer in both emission scenarios and periods. The variability in projected mean monthly  
477 precipitation among climate models indicates great uncertainty between GCMs (Figure 4a-d).  
478 The mean monthly temperature of all climate models clearly deviated from the baseline  
479 period (1981-2010), underlining the consistent change signal between GCMs (Figure 4e-h).  
480 The median of the 38 CMIP5 mean monthly precipitation data over the Goulburn-Broken  
481 Catchment in the RCP4.5 emission scenario showed declines in most of the months. The  
482 decreases were up to 6% in 2021–2050 (Figure 4a) and up to 11% in 2071–2100 (Figure 4c).  
483 Similarly, under the RCP8.5 emission scenario the median monthly precipitation, other than  
484 in January and February for both periods, showed decreases up to 7% in 2021–2050 (Figure  
485 4b) and up to 18% in 2071–2100 (Figure 4d). The simulations for January and February  
486 showed median increases of up to 4% and 5% respectively in 2071–2100 from the historical  
487 baseline. Some climate models projected very wet future climates while others projected  
488 relatively dry climates. There are relatively high uncertainties in the projected mean monthly  
489 precipitation results in summer when compared with the mean monthly precipitation in  
490 winter among the climates models.

491 In contrast to precipitation the projected mean monthly temperatures from all CMIP5 runs  
492 showed increases, the median of the mean monthly temperatures of all CMIP5 38 runs  
493 increased by about 0.8° C in winter and 1° C in summer in 2021–2050 (Figure 4e), and by  
494 about 1.3° C in winter and 1.8° C in summer in 2071–2100 (Figure 4g) under the RCP4.5  
495 scenario. Under the RCP8.5 emission scenario the temperatures increased by 1° C in winter  
496 and by 1.4° C in summer during 2021–2050 (Figure 4f) and by 2° C and 3° C in winter and  
497 summer respectively by the end of the 21<sup>st</sup> century (Figure 4h). After precipitation the second  
498 variable that drives water availability is potential evapotranspiration. Here PET is expected to  
499 increase among all CMIP5 runs as it is being driven solely by changes in temperature given  
500 that actual vapour pressure and solar radiation was also simulated as a function of

501 temperature. In the near future period (2021–2050) the median of all CMIP5 mean monthly  
502 reference evapotranspiration projections increase by 5% to 13% in both emission scenarios,  
503 with the largest change in winter and the smallest in summer. In the future period of 2071–  
504 2100, the mean monthly reference evapotranspiration increased by 7% in summer and 25% in  
505 winter under RCP4.5 emission scenarios, and by 10% in summer and 28% in winter under  
506 the RCP8.5 emission scenarios.

### 507 **3.3 Impact on LAI from change in climate**

#### 508 **3.3.1 Millennium drought**

509 The effects of the Millennium Drought (1997–2009) on modelled crop LAI were very severe  
510 with reductions in mean annual LAI between catchments of 38.1% to 48.0%, with a mean of  
511 42.7% (Table 2). The reduction in LAI of pasture was between 16.7% and 21.6% across the  
512 thirteen selected catchments with a spatial average of 19.4% (Table 2). The LAI of trees  
513 responded less than crop and pasture, and reductions were in the range 5.7% to 14.0%, with a  
514 spatial mean of 9.2% (Table 2). A significant reduction in each cover type also brought an  
515 overall decline in areal weighted sum of all land cover types LAI in the selected catchments  
516 which ranged from 5.8% to 17.9% (Table 2), which is similar to the reduction for trees,  
517 where tree is the dominant land cover type.

#### 518 **3.3.2 Future climate**

519 The changes in mean monthly LAI of crop, pasture and trees averaged over the whole  
520 Goulburn-Broken Catchment under future climates are vary between the CMIP5 runs and  
521 global warming scenarios. Averaged over all 38 CMIP5 runs, the near future (2021–2050)  
522 results for the study catchment showed that the mean annual LAI of cropland, pasture and  
523 trees declined up to 13%, 6.7% and 5.4% under the RCP4.5 scenarios, and by up to 16%, 8%  
524 and 6.6% under the RCP8.5 scenario (Table 3). A further reduction in the mean annual LAI  
525 of each land cover was simulated by the end of the 21<sup>st</sup> century for both emission scenarios  
526 (Table 3).

527 The effect of projected climate change on monthly total LAI (area weighted sum of all land  
528 cover types LAI) for the study catchments is given in (Figure 5). The median of the 38  
529 CMIP5 runs simulated mean monthly LAI showed declines in all three land cover types.  
530 Despite similar percentage changes in mean monthly precipitation and temperature forcing,  
531 the mean monthly total LAI across the catchment shows the largest decline in autumn and the  
532 smallest decline in spring during both future periods and scenarios. This difference reflects

533 the seasonality of moisture availability influencing plant growth. Based on the median of the  
534 38 CMIP5 runs, the predicted decline in the mean monthly LAI for crop, pasture and trees  
535 was 18.1%, 10.3% and 7.9% respectively in the period 2021–2050 (Figure 5a, e, i) and  
536 27.7%, 16.6% and 12.8% respectively in the period 2071–2100 under RCP4.5 (Figure 5c, g,  
537 k). Larger reductions were simulated under the RCP8.5 emission scenario with 21.4%, 12.7%  
538 and 9.5% in the period 2021–2050 (Figure 5b, f, j) and 36.5%, 22.5% and 17.9% respectively  
539 for crop, pasture and tree in the period 2071–2100 (Figure 5d, h, l).

### 540 **3.4 Impacts on runoff from change in climate**

#### 541 **3.4.1 Millennium drought**

542 The impact of the Millennium Drought on streamflow due to changes in precipitation and  
543 temperature alone and changes in precipitation and temperature and modelled LAI were  
544 simulated using the VIC model. The simulated reductions in mean annual streamflow during  
545 the Millennium Drought (1997–2009) as compared with the relatively normal period (1983–  
546 1995) across the selected catchments due to the change in climate alone ranged from 29.7%  
547 to 66.3% with a mean of 50% (Table 2). The reductions in LAI resulting from the decline in  
548 precipitation and increase in temperature increased mean annual streamflow by between 1.3%  
549 and 10.2% relative to the direct climate effect above (Table 2 and Figure 6).

#### 550 **3.4.2 Future climate**

551 The average of the 38 CMIP5 runs under the RCP4.5 scenario produced declines in mean  
552 annual runoff due to the change in precipitation and temperature alone ( $Q_{clim}$ ) that ranged  
553 from 6.8% to 20.3% in the period 2021–2050, and 11.5% to 30.1% for the period 2071–2100  
554 (Table 3 and Figure 7). For the higher emission scenario (RCP8.5), the reductions were a  
555 little larger-ranging from 8.3% to 23.3% in 2021–2050 and from 14.5% to 35.1% by the end  
556 the 21<sup>st</sup> century (Table 3 and Figure 6). The reductions in runoff due to climate are offset  
557 through the LAI effect ( $Q_{lai}$ ) that ranged from 2.3% to 27.7% and from 2.3% to 23.1% in the  
558 near and far future periods respectively under the RCP4.5 emission scenario. Similar offsets  
559 of 2.5% to 25.9% and 2.6% to 24.2% in the near and far future periods respectively were also  
560 found under the RCP8.5 emission scenario (Table 3 and Figure 7).

561 The differences between GCMs in terms of the net climate change impacts ( $CC + LAI$ ) on  
562 mean annual runoff and the LAI contribution to that effect are shown in Figure 8 and Figure  
563 9 respectively. While large uncertainty exists among the 38 CMIP5 runs, the median between  
564 the models showed declines in the net climate change ( $CC + LAI$ ) projections of mean annual

565 runoff in all catchments (Figure 8). The median decline in the mean annual runoff due to the  
566 net climate change impact was 15.3% and 26.7% in 2021–2050 and 2071–2100 respectively,  
567 under RCP4.5. A larger decline of 21.6% and 31.8% in 2021–2050 and 2071–2100  
568 respectively occurred under RCP8.5 (Figure 8). The simulated LAI effects of the climate  
569 change showed smaller variation between GCMs than the net climate change (*CC + LAI*)  
570 effect on mean annual runoff. The LAI effect works to offset the reduction in mean annual  
571 runoff resulting from lower precipitation and higher temperature. Figure 9 shows the  
572 magnitude of the LAI effect as a percentage of the magnitude of direct climate change effect  
573 (noting they work in opposite directions). The median of this across the 38 CMIP5 runs was  
574 up to 20%, depending on the month. The simulated LAI effect on mean annual runoff showed  
575 smaller variation between GCMs than the net climate change (*CC + LAI*) effect on mean  
576 annual runoff.

577 The direct climate change (*CC*) effect, the LAI effect of climate change and the net climate  
578 change (*CC+LAI*) effect on the mean monthly runoff for the selected catchments are given:  
579 Catchments 6 (Figure 10a, d, g, j), Catchment 10 (Figure 10b, e, h, k), and Catchment 11  
580 (Figure 10c, f, i, l). Catchments 6 and 10 are located in a high annual precipitation zone with  
581 trees as the dominant vegetation cover; whereas Catchment 11 is covered mostly with pasture  
582 and has relatively lower annual precipitation than Catchments 6 and 10. Depending on the  
583 month, for the 38 CMIP5 runs in 2021–2050 the median reduction in mean monthly runoff  
584 ( $Q_{net}$ ) were up to 10%, 24%, and 34% for catchment 6, 10, and 11, respectively for both the  
585 RCP4.5 and RCP8.5 scenarios (Figure 10). Further reductions projected by the end of the 21<sup>st</sup>  
586 century were up to 17%, 37% and 52% for catchments 6, 10, and 11, respectively, under both  
587 scenarios (Figure 10). Catchment 6 showed the lowest seasonality in the climate change  
588 effects for both emission scenarios and the LAI-related effects of climate change also showed  
589 the smallest seasonal variation. Catchment 11 runoff was the most impacted by projected  
590 climate changes and had the greatest benefit from LAI effects of climate change under both  
591 emission scenarios and future periods. The seasonal pattern of the LAI effect of climate  
592 change is similar under both RCP scenarios. The magnitude of this effect is relatively higher  
593 for drier projected future climates.

#### 594 **4 Discussion and Conclusion**

595 This study investigated the importance of incorporating the relationship between changing  
596 climate, in terms of precipitation and temperature, and vegetation LAI into a hydrological  
597 model to estimate changes in mean monthly and mean annual runoff under changing climatic  
598 conditions in the Goulburn-Broken Catchment, south-eastern Australia. A combination of  
599 VIC hydrological simulations with a simple model that relates climatic fluctuations with LAI  
600 for three different vegetation types revealed that 21<sup>st</sup> century climate change impacts on LAI  
601 significantly influence the projected runoff in the study catchments. LAIs of forest, pasture  
602 and crop were predicted to decline in the 21<sup>st</sup> century due to reductions in precipitation and  
603 increases in temperature.

604 Reduced LAI in response to a drier and warmer climate would reduce transpiration from  
605 vegetation and evaporative losses from canopy interception, which leaves the soil relatively  
606 wetter than if LAI response to climate was not included. This is important for runoff  
607 generation process as it promotes saturation excess runoff and subsurface flow, which are the  
608 dominant cause of runoff generation in the study region (Western et al., 1999). Previous  
609 studies in the region (Chiew et al., 2009; Chiew et al., 2011; Teng et al., 2012a; Teng et al.,  
610 2012b) concluded that runoff would decrease due to increases in evaporative demand and  
611 decreases in precipitation as a result of ongoing warming in the 21<sup>st</sup> century. However, the  
612 relationship between LAI and climate fluctuations was not taken into account in their  
613 modelling experiments. Therefore, in these studies the LAI effect is ignored and there is  
614 consequent overestimation of the runoff decline in the range of 2.3% to 27.7% (Figure 6 and  
615 Figure 7).

616 Projections of climate-induced vegetation dynamics and their hydrological impacts are  
617 influenced by various uncertainties that arise from using downscaled GCM outputs as inputs  
618 to the hydrologic model. These include large uncertainties in projections for precipitation  
619 from the various CMIP5 simulations (Teng et al., 2012b). In addition, the method used to  
620 downscale the GCM outputs really only captures changes the mean; however, any change in  
621 variability, which could have an effect on the projected future runoff, is ignored. The  
622 ensemble of 38 CMIP5 simulations from 15 GCMs was used to determine the range of  
623 uncertainty between GCMs. The results showed that the range of future climate projections  
624 from the various GCMs is wide, one climate model could project a very wet future climate  
625 while another a relatively dry climate. This suggests future analyses in other catchments  
626 should apply downscaled climate change scenarios from several CMIP5 runs from a range of

627 GCM models to the study area to get a sense of the possible range of climate change impact  
628 on both LAI and streamflow.

629 The results of this study illustrate that reduction of future precipitation and increase in mean  
630 temperature lead to reduction of runoff in a general sense. However, if the hydrologic model  
631 incorporated dynamic LAI information, as a function of changing climate, it would reduce  
632 the impact on runoff that comes from the climate alone. Reduction of LAI due to reduction of  
633 precipitation and increase in temperature decreases the evapotranspiration from vegetation  
634 and leaves the soil relatively wetter than if climate-induced changes in LAI were not  
635 represented in the modeling. The higher catchment moisture contents slightly increased  
636 runoff and partially offset the reduction in runoff due to changes in climate.

637 In interpreting the results presented here it is important to examine the assumptions that were  
638 made and the extent to which the results are dependent on those assumptions. Runoff  
639 processes can also triggered by other precipitation characteristics (intensity, duration, inter-  
640 storm duration) which have not been considered in this study. If inter-storm durations are  
641 expected to increase, this will alter the hydrologic fluxes even if the mean precipitation is  
642 maintained. However, the Climate–LAI model used in the study area (Tesemma et al., 2014)  
643 is related mainly to precipitation and potential evapotranspiration during the previous 6 to 9  
644 months. This limits the impact of changes in extreme precipitation characteristics in terms of  
645 modelling the Climate–LAI relationship. In order to satisfy the aim of this paper, which is to  
646 assess the impact of allowing LAI to respond to a changing climate, so long as the  
647 precipitation series is consistent between the runs with and without LAI responding to  
648 climate, we can assess the importance of the change in LAI on runoff simulation. Hence, in  
649 this study consideration of changing extreme precipitation events is less important; although  
650 it would be important for studies with the objective of predicting future floods or reservoir  
651 management.

652 Another assumption of [this study was](#) that the [impact on runoff](#) of rising atmospheric CO<sub>2</sub>  
653 concentrations, [via changes in](#) LAI and stomatal conductance, is [small relative](#) to the  
654 moisture availability effects. Therefore, here we assumed LAI responded [only](#) to precipitation  
655 and PET changes, not [changes in](#) CO<sub>2</sub>. Changes in atmospheric CO<sub>2</sub> concentrations could  
656 affect vegetation through increasing LAI and narrowing stomata (Ainsworth and Rogers,  
657 2007; Ewert, 2004; Warren et al., 2011). However, increased LAI may be limited by the  
658 availability of nutrients, particularly nitrogen (Fernández-Martínez et al., 2014; Körner,  
659 2006). Most of the results on this effect are derived from point experiments which could not

660 be extrapolated to the catchment scale where there is a complex interaction between soil,  
661 vegetation and climate. Increasing atmospheric CO<sub>2</sub> could also have two other effects on  
662 vegetation dynamics. First, biomass allocation may shift towards more above-ground plant  
663 structure (Obrist and Arnone, 2003), which implies more canopy leaf than active rooting area.  
664 This change could influence the water balance in either direction by increasing  
665 evapotranspiration due to interception losses or by decreasing evapotranspiration through  
666 limiting plant water uptake. Second, rising atmospheric CO<sub>2</sub> may favor C<sub>3</sub> species over C<sub>4</sub>  
667 species, which could lead to more woody plants compared to some grass species (Yu et al.,  
668 2014). This could influence the water balance by increasing evapotranspiration and  
669 decreasing runoff. In addition at the canopy scale, the evapotranspiration effect of increased  
670 LAI can be masked by shading among leaves, soil cover and raised canopy humidity  
671 (Hikosaka et al., 2005; Bunce, 2004). A study that considered both effects suggested that the  
672 fertilization effect of rising CO<sub>2</sub> is larger than the stomatal pore reduction effect, and the net  
673 effect is decreases in runoff (Piao et al., 2007). These two effects of increasing atmospheric  
674 CO<sub>2</sub> concentrations on vegetation work in opposite directions from a water balance  
675 perspective and may offset each other if they are close in magnitude (Gerten et al., 2008). In  
676 south-east Australia, it is known that vegetation growth is highly controlled by precipitation  
677 (water supply), and is less controlled by temperature and radiation (Nemani et al., 2003).  
678 Hence, most vegetation dynamics can be explained by variation in climate, which formed the  
679 basis of the LAI–Climate model developed in Tesemma et al. (2014). We acknowledge  
680 changing CO<sub>2</sub> levels could influence vegetation growth and water use efficiency and hence  
681 runoff, but we expect the impact on runoff to be smaller (Huntington, 2008; Uddling et al.,  
682 2008) than that due to changes in moisture state. Hence, exclusion of the fertilization and  
683 stomata suppression effects of rising atmospheric CO<sub>2</sub> on vegetation may not change the  
684 results significantly. However, the impact on runoff of CO<sub>2</sub> fertilization at the catchment  
685 scale remains an important area of on-going research.

686 A further assumption was that any effect of climate change on the spatial distribution of plant  
687 functional type (PFT) was ignored. That is the same spatial distribution of vegetation was  
688 used but with changed LAI. We acknowledge that changing climate (i.e increase in  
689 temperature) may shift the spatial distribution of PFTs, which has been reported in  
690 Mediterranean climate region (eg Lenihan et al., 2003; Crimmins et al., 2011). However, in  
691 our study area PFTs are largely determined by historical land use change (human activities)  
692 such as forest clearing for agriculture, rather than natural responses of vegetation to changed



693 climatic conditions. Therefore, future changes in the spatial distribution of agricultural crops  
694 and pastures are difficult to project as they are not solely due to climatic changes. In the  
695 forested areas, it is likely that issues that change water use such as changes in fire regime  
696 (Heath et al., 2014) and forest age (Cornish and Vertessy, 2001) would dominate over  
697 differences between species. Eucalyptus species already occupy high-altitude areas of the  
698 study catchment, which leaves little room for PFT changes due to up-slope migration in a  
699 warming climate. Most over-story trees in our study area are Eucalypts and while some  
700 movement of boundaries between dominant species may be expected, water use  
701 characteristics are likely to be relatively similar and there is insufficient information to  
702 represent species specific details of either migration or water use. Including these effects in  
703 the model may improve the results, but there is insufficient understanding at the granularity  
704 required to do so at present.

705 In summary, in this paper we use the VIC hydrological model to assess the impact on mean  
706 annual streamflow of ignoring climate induced changes in LAI for two changing climatic  
707 situations: (1) the recently observed “Millennium Drought”; and (2) for downscaled projected  
708 future climate change scenarios from 38 CMIP5 runs in the Goulburn-Broken catchment,  
709 Australia. In the Millennium Drought (1997–2009) not modelling the response of LAI to  
710 changing climatic variables led to further reduction in mean annual runoff, relative to the pre-  
711 drought period (1983–1995), of between 1.3% and 10.2% relative to modelling the dynamic  
712 response of LAI to decreased precipitation and increased temperature (Table 2 and Figure 6).  
713 For projected climate change under the RCP4.5 emission scenario ignoring the LAI response  
714 to changing climate could lead to a further reduction in mean annual runoff of between 2.3%  
715 and 27.7%, relative to the baseline period (1981–2010), in the near-term (2021–2050) and  
716 2.3% to 23.1% later in the century (2071–2100) relative to modelling the dynamic response  
717 of LAI to precipitation and temperature changes. Similar results (near-term 2.5% to 25.9%  
718 and end of century 2.6% to 24.2%) were found for climate change under the RCP8.5  
719 emission scenario (Table 3 and Figure 7). Due to the strong relationship between climatic  
720 variation and LAI, the Climate–LAI interaction should be included in hydrological models  
721 for improved climate change impact assessments and modelling under changing climatic  
722 conditions, particularly in arid and semi-arid regions where vegetation is strongly influenced  
723 by climate.

724 **Acknowledgements**

725 This study was funded by the Australian Research Council (ARC) (Project Nos: ARC  
726 LP100100546, ARC FT130100274 and ARC FT120100130), the Natural Science Foundation  
727 of China (Project No: 91125007) and the Commonwealth of Australia under the Australia  
728 China Science and Research Fund (Project No: ACSRF800). We would like to thank the  
729 University of Melbourne for providing a scholarship to the first author. We thank editor  
730 Ciaran Harmon and two anonymous reviewers for comments that improved this manuscript.

731 **References**

- 732 Ainsworth, E. A., and Rogers, A.: The response of photosynthesis and stomatal conductance  
733 to rising [CO<sub>2</sub>]: mechanisms and environmental interactions, *Plant, Cell & Environment*, 30,  
734 258-270, 10.1111/j.1365-3040.2007.01641.x, 2007.
- 735 Allen, R. G., Pereira, L.S., Raes, D., and Smith, M.: Crop evapotranspiration Guidelines for  
736 computing crop water requirements, FAO Irrigation and Drainage Paper 56, Food and  
737 Agriculture Organization of the United Nations, 1998.
- 738 Bunce, J. A.: Carbon dioxide effects on stomatal responses to the environment and water use  
739 by crops under field conditions, *Oecologia*, 140, 1-10, 10.1007/s00442-003-1401-6, 2004.
- 740 Cai, W., and Cowan, T.: Evidence of impacts from rising temperature on inflows to the  
741 Murray-Darling Basin, *Geophys. Res. Lett.*, 35, L07701, 10.1029/2008GL033390, 2008.
- 742 Chiew, F. H. S., Teng, J., Vaze, J., Post, D. A., Perraud, J. M., Kirono, D. G. C., and Viney,  
743 N. R.: Estimating climate change impact on runoff across southeast Australia: Method,  
744 results, and implications of the modeling method, *Water Resour. Res.*, 45, W10414,  
745 10.1029/2008WR007338, 2009.
- 746 Chiew, F. H. S., Young, W. J., Cai, W., and Teng, J.: Current drought and future  
747 hydroclimate projections in southeast Australia and implications for water resources  
748 management, *Stochastic Environmental Research and Risk Assessment*, 25, 601-612,  
749 10.1007/s00477-010-0424-x, 2011.
- 750 Chiew, F. H. S., Potter, N. J., Vaze, J., Petheram, C., Zhang, L., Teng, J., and Post, D. A.:  
751 Observed hydrologic non-stationarity in far south-eastern Australia: implications for  
752 modelling and prediction, *Stochastic Environmental Research and Risk Assessment*, 28, 3-15,  
753 10.1007/s00477-013-0755-5, 2014.
- 754 Cornish, P. M., and Vertessy, R. A.: Forest age-induced changes in evapotranspiration and  
755 water yield in a eucalypt forest, *J. Hydrol.*, 242, 43-63, 10.1016/S0022-1694(00)00384-X,  
756 2001.
- 757 Crimmins, S. M., Dobrowski, S. Z., Greenberg, J. A., Abatzoglou, J. T., and Mynsberge, A.  
758 R.: Changes in climatic water balance drive downhill shifts in plant species' optimum  
759 elevations. *Science*, 331(6015), 324-327, 2011.

760 Cuo, L., Zhang, Y., Gao, Y., Hao, Z., and Cairang, L.: The impacts of climate change and  
761 land cover/use transition on the hydrology in the upper Yellow River Basin, China, *J.*  
762 *Hydrol.*, 502, 37-52, <http://dx.doi.org/10.1016/j.jhydrol.2013.08.003>, 2013.

763 Demaria, E. M., Nijssen, B., and Wagener, T.: Monte Carlo sensitivity analysis of land  
764 surface parameters using the Variable Infiltration Capacity model, *J. Geophys. Res.-Atmos.*,  
765 112, D11113, doi:10.1029/2006JD007534, 2007.

766 Ellis, T. W., and Hatton, T. J.: Relating leaf area index of natural eucalypt vegetation to  
767 climate variables in southern Australia, *Agric. Water Manage.*, 95, 743-747,  
768 <http://dx.doi.org/10.1016/j.agwat.2008.02.007>, 2008.

769 Ewert, F.: Modelling Plant Responses to Elevated CO<sub>2</sub>: How Important is Leaf Area Index?,  
770 *Annals of Botany*, 93, 619-627, 10.1093/aob/mch101, 2004.

771 Food and Agriculture Organization of the United Nations (FAO): Digital soil map of the  
772 world, Version 3.5. FAO, Rome, Italy, 1995.

773 Fernández-Martínez, M., Vicca, S., Janssens, I., Sardans, J., Luysaert, S., Campioli, M.,  
774 Chapin III, F., Ciais, P., Malhi, Y., and Obersteiner, M.: Nutrient availability as the key  
775 regulator of global forest carbon balance, *Nature Climate Change*, 4, 471-476, 2014.

776 Fowler, H. J., Blenkinsop, S., and Tebaldi, C.: Linking climate change modelling to impacts  
777 studies: recent advances in downscaling techniques for hydrological modelling, *Int. J.*  
778 *Climatol.*, 27, 1547-1578, 10.1002/joc.1556, 2007.

779 Ford, T. W., and Quiring, S. M.: Influence of MODIS-Derived Dynamic Vegetation on VIC-  
780 Simulated Soil Moisture in Oklahoma, *J. Hydrometeorol.*, 14, 1910-1921, doi:10.1175/JHM-  
781 D-13-037.1, 2013.

782 Geoscience Australia: GEODATA 9 Second Digital Elevation Model (DEM-9S) Version 3,  
783 available at: [http://www.ga.gov.au/metadata-gateway/metadata/record/gcat\\_66006](http://www.ga.gov.au/metadata-gateway/metadata/record/gcat_66006) (last  
784 accessed: 20 december 2013), 2008.

785 Gerten, D., Rost, S., von Bloh, W., and Lucht, W.: Causes of change in 20th century global  
786 river discharge, *Geophys. Res. Lett.*, 35, L20405, 10.1029/2008GL035258, 2008.

787 Harrold, T. I., Jones, R. N., and Watterson, I. G.: Applying climate changes simulated by  
788 GCMs to the generation of fine-scale rainfall scenarios, *Hydro 2005*, 29<sup>th</sup> Hydrology and  
789 Water Resources Symposium, Canberra, 2005.

790 Heath, J. T., Chafer, C. J., van Ogtrop, F. F., and Bishop, T. F. A.: Post-wildfire recovery of  
791 water yield in the Sydney Basin water supply catchments: An assessment of the 2001/2002  
792 wildfires, *J. Hydrol.*, 519, 1428-1440, 10.1016/j.jhydrol.2014.09.033, 2014.

793 Hikosaka, K., Onoda, Y., Kinugasa, T., Nagashima, H., Anten, N. P. R., and Hirose, T.: Plant  
794 responses to elevated CO<sub>2</sub> concentration at different scales: leaf, whole plant, canopy, and  
795 population, *Ecological Research*, 20, 243-253, 10.1007/s11284-005-0041-1, 2005.

796 Hughes, J. D., Petrone, K. C., and Silberstein, R. P.: Drought, groundwater storage and  
797 stream flow decline in southwestern Australia, *Geophys. Res. Lett.*, 39, L03408,  
798 10.1029/2011GL050797, 2012.

799 Huntington, T. G.: CO<sub>2</sub>-induced suppression of transpiration cannot explain increasing  
800 runoff, *Hydrol. Processes*, 2008.

801 Jahan, N., and Gan, T. Y.: Modelling the vegetation–climate relationship in a boreal  
802 mixedwood forest of Alberta using normalized difference and enhanced vegetation indices,  
803 *Int. J. Remote Sens.*, 32, 313-335, 10.1080/01431160903464146, 2011.

804 Jones, D. A., Wang, W., and Fawcett, R.: High-quality spatial climate data-sets for Australia,  
805 *Australian Meteorological and Oceanographic Journal*, 58, 233-248, 2009.

806 Kalma, J. D., Bates, B. C., and Woods, R. A.: Predicting catchment-scale soil moisture status  
807 with limited field measurements, *Hydrol. Process.*, 9, 445-467, doi:10.1002/hyp.3360090315,  
808 1995.

809 Kimball, J. S., Running, S. W., and Nemani, R. R.: An improved method for estimating  
810 surface humidity from daily minimum temperature, *Agr. Forest Meteorol.*, 85, 87-98, 1997.

811 Körner, C.: Plant CO<sub>2</sub> responses: an issue of definition, time and resource supply, *New*  
812 *Phytol*, 172, 393-411, 10.1111/j.1469-8137.2006.01886.x, 2006.

813 Lenihan, J. M., Drapek, R., Bachelet, D., and Neilson, R. P.: Climate change effects on  
814 vegetation distribution, carbon, and fire in California. *Ecological Applications*, 13(6), 1667-  
815 1681, 2003.

816 Liang, X., Wood, E. F., and Lettenmaier, D. P.: Surface soil moisture parameterization of the  
817 VIC-2L model: Evaluation and modification, *Global Planet. Change*, 13, 195-206,  
818 doi:10.1016/0921-8181(95)00046-1, 1996.

819 Lockart, N., Kavetski, D., and Franks, S. W.: On the recent warming in the Murray-Darling  
820 Basin: Land surface interactions misunderstood, *Geophys. Res. Lett.*, 36, L24405,  
821 10.1029/2009GL040598, 2009.

822 McMahon, T. A., Peel, M. C., and Karoly, D. J.: Assessment of precipitation and temperature  
823 data from CMIP3 global climate models for hydrologic simulation, *Hydrol. Earth Syst. Sci.*,  
824 19, 361-377, 2015.

825 McVicar, T. R., Van Niel, T. G., Li, L. T., Roderick, M. L., Rayner, D. P., Ricciardulli, L.,  
826 and Donohue, R. J.: Wind speed climatology and trends for Australia, 1975–2006: Capturing  
827 the stilling phenomenon and comparison with near-surface reanalysis output, *Geophys. Res.*  
828 *Lett.*, 35, L20403, doi:10.1029/2008GL035627, 2008.

829 Meinshausen, M., Smith, S. J., Calvin, K., Daniel, J. S., Kainuma, M. L. T., Lamarque, J. F.,  
830 Matsumoto, K., Montzka, S. A., Raper, S. C. B., Riahi, K., Thomson, A., Velders, G. J. M.,  
831 and van Vuuren, D. P. P.: The RCP greenhouse gas concentrations and their extensions from  
832 1765 to 2300, *Clim. Change*, 109, 213-241, 10.1007/s10584-011-0156-z, 2011.

833 Milly, P. C. D., Dunne, K. A., and Vecchia, A. V.: Global pattern of trends in streamflow and  
834 water availability in a changing climate, *Nature*, 438, 347-350, 2005.

835 Moss, R. H., Edmonds, J. A., Hibbard, K. A., Manning, M. R., Rose, S. K., van Vuuren, D.  
836 P., Carter, T. R., Emori, S., Kainuma, M., Kram, T., Meehl, G. A., Mitchell, J. F. B.,  
837 Nakicenovic, N., Riahi, K., Smith, S. J., Stouffer, R. J., Thomson, A. M., Weyant, J. P., and  
838 Wilbanks, T. J.: The next generation of scenarios for climate change research and assessment,  
839 *Nature*, 463, 747-756, 10.1038/nature08823, 2010.

840 Moriasi, D. N., Arnold, J. G., Van Liew, M. W., Bingner, R. L., Harmel, R. D., and Veith, T.  
841 L.: Model evaluation guidelines for systematic quantification of accuracy in watershed  
842 simulations, *T. ASABE*, 50, 885-900, 2007.

843 Murray, S. J., Foster, P. N., and Prentice, I. C.: Evaluation of global continental hydrology as  
844 simulated by the Land-surface Processes and eXchanges Dynamic Global Vegetation Model,  
845 *Hydrol. Earth Syst. Sci.*, 15, 91-105, 10.5194/hess-15-91-2011, 2011.

846 Murray, S. J., Foster, P. N., and Prentice, I. C.: Future global water resources with respect to  
847 climate change and water withdrawals as estimated by a dynamic global vegetation model, *J.*  
848 *Hydrol.*, 448–449, 14-29, <http://dx.doi.org/10.1016/j.jhydrol.2012.02.044>, 2012a.

849 Murray, S. J., Watson, I. M., and Prentice, I. C.: The use of dynamic global vegetation  
850 models for simulating hydrology and the potential integration of satellite observations, *Prog.*  
851 *Phys. Geog.*, 10.1177/0309133312460072, 2012b.

852 Nemani, R. R., Keeling C. D., Hashimoto, H., Jolly, W. M., Piper, S. C., Tucker, C. J.,  
853 Myneni, R. B., Running, S. W.: Climate-driven increases in global terrestrial net primary  
854 production from 1982 to 1999, *Science*, 300, 1560-1563, 2003.

855 O'Grady, A. P., Carter, J. L., and Bruce, J.: Can we predict groundwater discharge from  
856 terrestrial ecosystems using existing eco-hydrological concepts?, *Hydrol. Earth Syst. Sci.*, 15,  
857 3731-3739, 10.5194/hess-15-3731-2011, 2011.

858 Obrist, D., and Arnone, J. A.: Increasing CO<sub>2</sub> accelerates root growth and enhances water  
859 acquisition during early stages of development in *Larrea tridentate*. *New Phytol.* 159:175–  
860 184. doi:10.1046/j.1469-8137.2003.00791.x, 2003.

861 Palmer, A. R., Fuentes, S., Taylor, D., Macinnis-Ng, C., Zeppel, M., Yunusa, I., and Eamus,  
862 D.: Towards a spatial understanding of water use of several land-cover classes: an  
863 examination of relationships amongst pre-dawn leaf water potential, vegetation water use,  
864 aridity and MODIS LAI, *Ecohydrology*, 3, 1-10, 10.1002/eco.63, 2010.

865 Peel, M. C., and Blöschl, G.: Hydrological modelling in a changing world, *Prog. Phys. Geog.*,  
866 35, 249-261, 10.1177/0309133311402550, 2011.

867 Piao, S., Friedlingstein, P., Ciais, P., de Noblet-Ducoudré, N., Labat, D., and Zaehle, S.:  
868 Changes in climate and land use have a larger direct impact than rising CO<sub>2</sub> on global river  
869 runoff trends, *Proceedings of the National Academy of Sciences*, 104, 15242-15247,  
870 10.1073/pnas.0707213104, 2007.

871 Potter, N. J., and Chiew, F. H. S.: An investigation into changes in climate characteristics  
872 causing the recent very low runoff in the southern Murray-Darling Basin using rainfall-runoff  
873 models, *Water Resour. Res.*, 47, W00G10, 10.1029/2010WR010333, 2011.

874 Roderick, M. L., and Farquhar, G. D.: A simple framework for relating variations in runoff to  
875 variations in climatic conditions and catchment properties, *Water Resour. Res.*, 47, W00G07,  
876 10.1029/2010WR009826, 2011.

877 Scheiter, S., Langan, L., and Higgins S. I.: Next-generation dynamic global vegetation  
878 models: learning from community ecology. *New Phytologist* 198: 957–969, 2013.

879 Schenk, H. J. and Jackson, R. B.: The global biogeography of roots, *Ecological Monographs*,  
880 72, 311–328, 2002.

881 Taylor, K. E., Stouffer, R. J., and Meehl, G. A.: An Overview of CMIP5 and the Experiment  
882 Design, *Bull. Am. Meteorol. Soc.*, 93, 485-498, 10.1175/BAMS-D-11-00094.1, 2012.

883 Teng, J., Chiew, F. H. S., Vaze, J., Marvanek, S., and Kirono, D. G. C.: Estimation of  
884 Climate Change Impact on Mean Annual Runoff across Continental Australia Using Budyko  
885 and Fu Equations and Hydrological Models, *Journal of Hydrometeorology*, 13, 1094-1106,  
886 10.1175/JHM-D-11-097.1, 2012a.

887 Teng, J., Vaze, J., Chiew, F. H. S., Wang, B., and Perraud, J.-M.: Estimating the Relative  
888 Uncertainties Sourced from GCMs and Hydrological Models in Modeling Climate Change  
889 Impact on Runoff, *J. Hydrometeorol.*, 13, 122-139, 10.1175/JHM-D-11-058.1, 2012b.

890 Tesemma, Z. K., Wei, Y., Western, A. W., and Peel, M. C.: Leaf area index variation for  
891 cropland, pasture and tree in response to climatic variation in the Goulburn-Broken  
892 catchment, Australia, *J. Hydrometeorol.*, 10.1175/JHM-D-13-0108.1, 2014a.

893 Thornton, P. E., and Running S. W.: An improved algorithm for estimating incident daily  
894 solar radiation from measurements of temperature, humidity, and precipitation, *Agr. Forest  
895 Meteorol.*, 93, 211-228, 1999.

896 Uddling, J., Teclaw, R. M., Kubiske, M. E., Pregitzer, K. S., and Ellsworth, D. S.: Sap flux in  
897 pure aspen and mixed aspen–birch forests exposed to elevated concentrations of carbon  
898 dioxide and ozone, *Tree Physiol.*, 28, 1231-1243, 2008.

899 Vaze, J., Post, D. A., Chiew, F. H. S., Perraud, J. M., Viney, N. R., and Teng, J.: Climate  
900 non-stationarity - Validity of calibrated rainfall-runoff models for use in climate change  
901 studies, *J. Hydrol.*, 394, 447 - 457, 10.1016/j.jhydrol.2010.09.018, 2010.

902 Vaze, J., and Teng, J.: Future climate and runoff projections across New South Wales,  
903 Australia: results and practical applications, *Hydrol. Processes*, 25, 18-35, 10.1002/hyp.7812,  
904 2011.

905 Verdon-Kidd, D. C., and Kiem, A. S.: Nature and causes of protracted droughts in southeast  
906 Australia: Comparison between the Federation, WWII, and Big Dry droughts, *Geophys. Res.  
907 Lett.*, 36, L22707, 10.1029/2009GL041067, 2009.



908 Vuuren, D. P., Edmonds, J., Kainuma, M., Riahi, K., Thomson, A., Hibbard, K., Hurtt, G. C.,  
909 Kram, T., Krey, V., Lamarque, J.-F., Masui, T., Meinshausen, M., Nakicenovic, N., Smith, S.  
910 J., and Rose, S. K.: The representative concentration pathways: an overview, *Clim. Change*,  
911 109, 5-31, 2011.

912 Warren, J. M., Norby, R. J., and Wullschleger, S. D.: Elevated CO<sub>2</sub> enhances leaf senescence  
913 during extreme drought in a temperate forest, *Tree Physiol.*, 10.1093/treephys/tpq002, 2011.

914 Western, A. W., Grayson, R. B., and Green, T. R.: The Tarrawarra project: high resolution  
915 spatial measurement, modelling and analysis of soil moisture and hydrological response,  
916 *Hydrol. Processes*, 13, 633-652, 10.1002/(SICI)1099-1085(19990415)13:5<633::AID-  
917 HYP770>3.0.CO;2-8, 1999.

918 White, D. A., Battaglia, M., Mendham, D. S., Crombie, D. S., Kinal, J. O. E., and McGrath,  
919 J. F.: Observed and modelled leaf area index in *Eucalyptus globulus* plantations: tests of  
920 optimality and equilibrium hypotheses, *Tree Physiol.*, 30, 831-844, 10.1093/treephys/tpq037,  
921 2010.

922 Wullschleger, S. D., Epstein, H. E., Box, E. O., Euskirchen, E. S., Goswami, S., Iversen, C.  
923 M., Kattge, J., Norby, R. J., van Bodegom, P. M., Xu, X.: Plant functional types in Earth  
924 System Models: past experiences and future directions for application of dynamic vegetation  
925 models in high-latitude ecosystems. *Annals of Botany* 114: 1–16, 2014.

926 Yapo, P. O., Gupta, H. V., and Sorooshian, S.: Multi-objective global optimization for  
927 hydrologic models, *J. Hydrol.*, 204, 83-97, doi:10.1016/S0022-1694(97)00107-8, 1998.

928 Yu, M., Wang, G., Parr, D., and Ahmed, K.: Future changes of the terrestrial ecosystem  
929 based on a dynamic vegetation model driven with RCP8.5 climate projections from 19  
930 GCMs, *Clim. Change*, 127, 257-271, 10.1007/s10584-014-1249-2, 2014.

931 Zhao, F., Chiew, F. H. S., Zhang, L., Vaze, J., Perraud, J.-M., and Li, M.: Application of a  
932 macroscale hydrologic model to estimate streamflow across southeast Australia, *J.*  
933 *Hydrometeorol.*, 13, 1233-1250, doi:10.1175/jhm-d-11-0114.1, 2012a.

934 Zhao, F. F., Xu, Z. X., and Zhang, L.: Changes in streamflow regime following vegetation  
935 changes from paired catchments, *Hydrol. Processes*, 26, 1561-1573, 10.1002/hyp.8266,  
936 2012b.

937

938 **List of tables**

939 [Table 1 Calibrated model parameters and model performance during calibration \(1982–1997\)](#)  
940 [and evaluation \(1998–2012\) periods.](#)

941 Table 2. Vegetation type distributions for each catchment and changes in mean annual  
942 precipitation, temperature, LAI and streamflow during the Millennium Drought (1997–2009)  
943 relative to (1983–1995).

944 Table 3. Impacts on mean annual precipitation, temperature, LAI and streamflow of projected  
945 climate change averaged over 38 CMIP5 runs relative to (1981–2010).

946 **List of figures**

947 Figure 1. Location map of the study area (a), dryness index (mean annual reference  
948 evapotranspiration divided by mean annual precipitation) (b) and land cover type (c).

949 Figure 2. Long-term mean monthly climate observations plotted with the 38 CMIP5 runs  
950 during the baseline period (1980–2010) for Goulburn-Broken Catchment (a) long-term mean  
951 monthly precipitation (b) long-term mean monthly maximum temperature and (c) long-term  
952 mean monthly minimum temperature.

953 Figure 3. Flowchart showing the modelling experiments and calculation of effects: CC effect  
954 indicates the climate change effect of precipitation and temperature with unchanged LAI, CC  
955 + LAI effect indicates the climate change effect of precipitation, temperature and leaf area  
956 index.

957 Figure 4. Box plots of percentage changes in the mean monthly precipitation (a, b, c, d) and  
958 changes in mean monthly temperatures (e, f, g, h) in the Goulburn-Broken Catchment for the  
959 future periods 2021–2050 and 2071–2100 for the 38 CMIP5 runs of climate projections.  
960 Changes are relative to the historical (1981–2010) mean monthly precipitation and  
961 temperatures. The lower boundary of the box indicates the 25th percentile, a line within the  
962 box marks the median, and the upper boundary of the box indicates the 75th percentile and  
963 the whiskers are delimited by the maximum and minimum.

964 Figure 5. Box plots of changes in mean monthly LAI derived from the 38 CMIP5 runs for  
965 climate projections during 2021–2050 and 2071–2100 under RCP4.5 and RCP8.5 scenarios  
966 for crop (a, b, c, d); pasture (e, f, g, h) and tree (i, j, k, l) in the Goulburn-Broken Catchment.  
967 Changes are relative to LAI calculated using climate time series for the 1981–2010 baseline.  
968 The lower boundary of the box indicates the 25th percentile, a line within the box marks the  
969 median, and the upper boundary of the box indicates the 75th percentile and the whiskers are  
970 delimited by the maximum and minimum.

971 Figure 6. Impacts on catchment mean annual streamflow of the Millennium drought (1997–  
972 2009) relative to the period 1983–1995. CC effect indicates precipitation and temperature  
973 effect with unchanged LAI; CC + LAI effect indicates precipitation, temperature and LAI  
974 effect. The proportional LAI effect indicates the LAI effect as a percentage of the CC effect.

975 Figure 7. Impact on catchment mean annual streamflow average over the 38CMIP5 runs of  
976 projected climate change for the future periods 2021–2050 and 2071–2100 under RCP4.5 (a,  
977 b) and RCP8.5 (c, d), relative to the 1981–2010 base period. CC effect indicates precipitation

978 and temperature effect with unchanged LAI; CC + LAI effect indicates precipitation,  
979 temperature and LAI effect. The proportional LAI effect indicates the LAI effect as a  
980 percentage of the CC effect.

981 Figure 8. Box plots of the net climate change (CC + LAI) effect on mean annual runoff  
982 during (2021–2050, 2071–2100) under RCP4.5 (a, b) and RCP8.5 (c, d) emission scenarios  
983 from each of the 38 CMIP5 runs. Changes are relative to the historical (1981–2010) period.  
984 The lower boundary of the box indicates the 25th percentile, a line within the box marks the  
985 median, and the upper boundary of the box indicates the 75th percentile and the whiskers are  
986 delimited by the maximum and minimum.

987 Figure 9. Box plots of contribution of LAI to the climate change effect on mean annual runoff  
988 for future (2021–2050, 2071–2100) climate forcing under RCP4.5 (a, b) and RCP8.5 (c, d)  
989 emission scenarios from each of the 38 CMIP5 runs as compared to the historical (1981–  
990 2010) period. The LAI effect is normalized by the effect of precipitation and temperature  
991 with unchanged LAI (i.e. CC effect) and expressed as a percentage. The lower boundary of  
992 the box indicates the 25th percentile, a line within the box marks the median, and the upper  
993 boundary of the box indicates the 75th percentile and the whiskers are delimited by the  
994 maximum and minimum.

995 Figure 10. Box plots of impacts on mean monthly streamflow from 38 CMIP5 runs of  
996 catchment 6 (a, d, g and j), catchment 10 (b, e, h and k), and catchment 11 (c, f, i and l) of  
997 projected climate change for future periods (2021–2050) and (2071–2100) under RCP4.5 and  
998 RCP8.5 respectively relative to the 1981–2010 base period. CC effect indicates precipitation  
999 and temperature effect with unchanged LAI; CC + LAI effect indicates precipitation,  
1000 temperature and LAI effect. The lower boundary of the box indicates the 25th percentile, a  
1001 line within the box marks the median, and the upper boundary of the box indicates the 75th  
1002 percentile and the whiskers are delimited by the maximum and minimum.

1003

1004 Table 1 Calibrated model parameters and model performance during calibration (1982–1997)  
 1005 and evaluation (1998–2012) periods.

ID	River and station name	Model parameters							Calibration (1982-1997)			Evaluation (1998-2012)		
		b	Ds	Ws	d2	d3	Dsmax	exp	Nash (%)	logNash (%)	Bias (%)	Nash (%)	logNash (%)	Bias (%)
1	Moonee Creek @ Lima	0.149	0.598	0.170	1.99	0.47	0.13	2.98	82.7	80.2	2.2	86.1	78.1	8.0
2	Delatite River @ Tonga Bridge	0.062	0.014	0.755	0.81	1.88	0.30	2.95	82.7	91.9	6.4	84.2	89.4	-5.4
3	Howqua River @ Glan Esk	0.244	0.291	0.006	1.65	0.28	11.60	1.15	90.4	89.4	-2.5	89.3	90.3	-0.8
4	Goulburn River @ Dohertys	0.206	0.891	0.035	1.43	0.45	22.01	1.42	95.9	91.0	2.2	92.4	90.8	-2.4
5	Big river @ Jamieson	0.183	0.610	0.736	1.70	0.81	0.01	2.19	89.7	86.5	8.9	81.5	85.7	11.9
6	Rubicon River @ Rubicon	0.216	0.059	0.200	0.52	1.77	19.29	1.28	93.8	94.9	-2.4	87.4	92.0	3.4
7	Acheron River @ Taggerty Murrindindi River @ above	0.168	0.030	0.293	1.97	1.84	0.16	2.59	82.6	85.8	9.5	82.4	84.4	-2.4
8	colwells	0.130	0.801	0.297	1.97	1.89	1.11	2.67	68.9	62.8	14.6	79.7	84.7	3.9
9	Yea river @ Devlins Bridge	0.072	0.428	0.646	1.93	1.27	0.05	2.99	79.8	78.3	26.4	68.0	69.3	34.1
10	King Parrot Creek @ Flowerdale	0.071	0.041	0.665	0.71	1.95	0.73	2.87	61.5	66.1	45.8	73.0	62.6	41.1
11	Sugarloaf Creek @ Ash Bridge	0.001	0.592	0.804	1.31	1.18	0.00	1.39	78.6	73.4	-3.5	59.0	40.0	127.5
12	Hughes Creek @ Tarcombe road	0.043	0.215	0.514	1.04	1.88	0.07	3.20	82.5	89.3	9.2	62.7	58.9	39.2
13	Home Creek @ Yarck	0.0004	0.415	0.524	0.66	1.91	0.01	2.97	81.7	87.1	-12.7	75.6	64.7	30.7

1006

1007

1008 Table 2. Vegetation type distributions for each catchment and changes in mean annual  
 1009 precipitation, temperature, LAI and streamflow during the Millennium Drought (1997–2009)  
 1010 relative to (1983–1995).

Catchments ID													
Variables*	1	2	3	4	5	6	7	8	9	10	11	12	13
Crop cover (%)	0.6	1.0									1.5	1.2	1.2
Pasture cover (%)	14.4	32.7	3.3	6.4	0.92	5.5	9.94	2.57	25.9	7.62	63.5	56.3	48.8
Tree cover (%)	85.0	66.3	96.7	93.6	99.1	94.5	90.1	97.4	74.1	92.4	35	42.6	50.1
P (%)	-23.2	-23.6	-21.1	-18.0	-17.9	-21.0	-20.1	-20.1	-19.4	-21.7	-19.5	-22.6	-24.1
T (°C)	0.2	0.3	0.3	0.4	0.4	0.3	0.3	0.2	0.3	0.2	0.3	0.3	0.3
LAI crop (%)	-44.2	-48.0									-38.1	-41.8	-41.4
LAI pasture (%)	-20.5	-21.6	-19.5	-16.9	-16.7	-18.7	-19.0	-19.1	-19.5	-19.7	-19.6	-20.2	-20.8
LAI tree (%)	-11.4	-10.3	-8.2	-6.6	-5.7	-5.9	-7.0	-6.3	-9.1	-9.2	-14.0	-12.5	-13.9
LAI total (%)	-12.9	-14.4	-8.6	-7.3	-5.8	-6.6	-8.2	-6.6	-11.8	-10.0	-17.9	-17.2	-17.6
Q <sub>clim</sub> (%)	-49.3	-61.5	-43.7	-39.1	-42.9	-29.7	-44.0	-41.2	-55.2	-57.1	-66.3	-61.8	-57.9
Q <sub>net</sub> (%)	-48.0	-59.7	-42.8	-38.3	-42.3	-29.3	-43.2	-40.6	-53.3	-55.2	-61.4	-56.1	-53.2
Q <sub>lai</sub> (%)	2.6	3.0	2.1	2.1	1.5	1.3	1.9	1.4	3.6	3.4	8.0	10.2	8.9

1011 \* P (%) is the change in mean annual precipitation in percentage, T (°C) is the change in mean annual temperature in Degree Celsius, Q<sub>clim</sub>  
 1012 indicates the climate effect on runoff, Q<sub>net</sub> is the net effect of climate and LAI on runoff and Q<sub>lai</sub> is proportion of the climate effect (Q<sub>clim</sub>)  
 1013 that is offset by the LAI effect.

1014

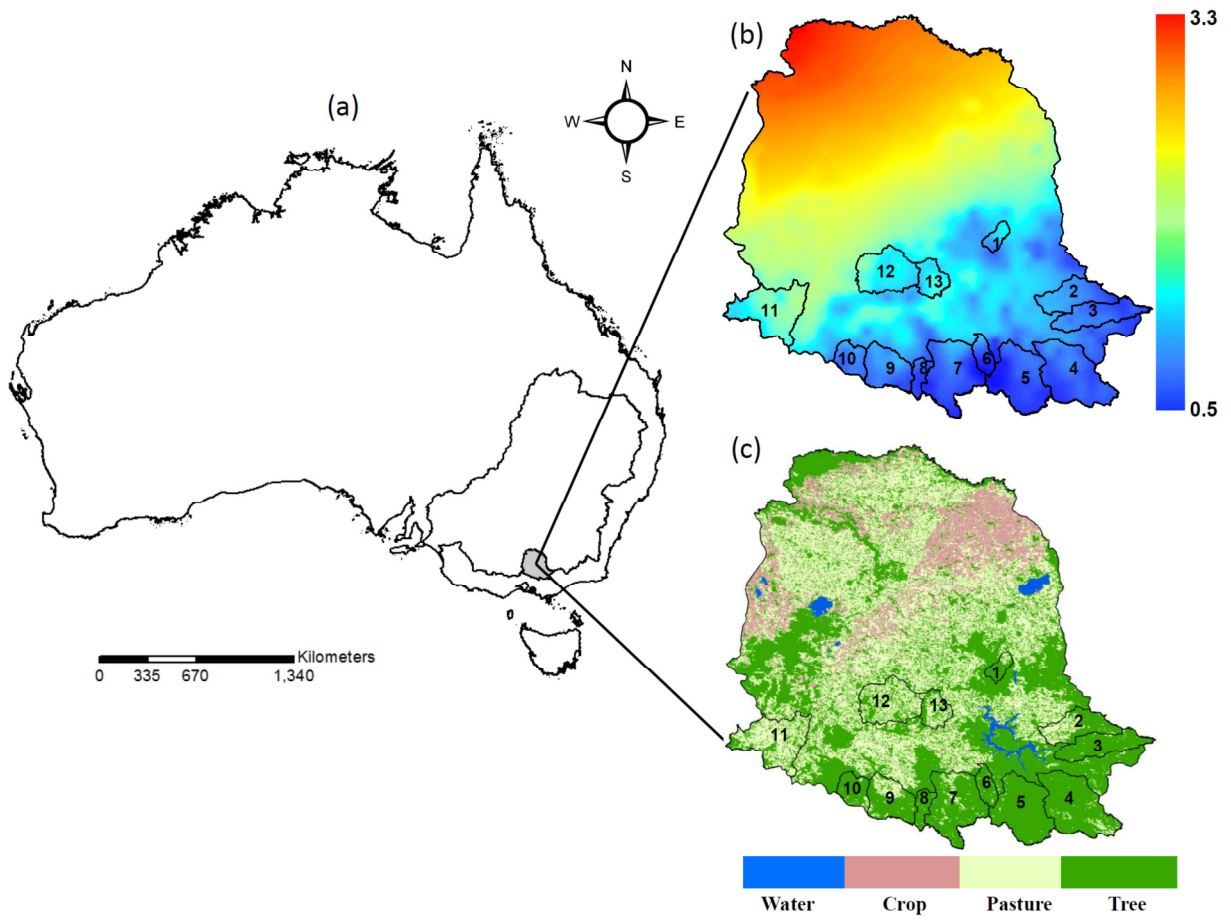
1015 Table 3. Impacts on mean annual precipitation, temperature, LAI and streamflow of projected  
 1016 climate change averaged over 38 CMIP5 runs relative to (1981–2010).

Catchments ID															
Periods	Variables*	1	2	3	4	5	6	7	8	9	10	11	12	13	
2021-2050 RCP4.5	P (%)	-2.9	-2.9	-2.9	-2.9	-2.9	-2.9	-2.9	-2.9	-2.9	-2.9	-2.9	-2.9	-2.9	
	T (°C)	0.9	0.9	0.9	0.9	0.9	0.9	0.9	0.9	0.9	0.9	0.9	0.9	0.9	
	LAI crop (%)	-12.9	-13.0										-12.9	-13.0	-12.8
	LAI pasture (%)	-5.9	-5.6	-5.4	-5.6	-5.3	-4.8	-5.4	-5.4	-6.1	-6.1	-6.7	-6.3	-6.3	
	LAI tree (%)	-3.9	-2.9	-2.5	-2.4	-2.0	-1.7	-2.1	-1.9	-3.0	-3.0	-5.4	-4.6	-4.8	
	LAI total (%)	-4.2	-3.9	-2.6	-2.6	-2.0	-1.8	-2.5	-1.9	-3.8	-3.2	-6.3	-5.6	-5.7	
	Q <sub>clim</sub> (%)	-12.3	-17.6	-11.4	-11.5	-13.5	-6.8	-12.4	-12.6	-17.4	-18.4	-20.3	-18.9	-14.2	
	Q <sub>net</sub> (%)	-11.4	-16.3	-10.9	-11.1	-13.2	-6.6	-11.9	-12.2	-15.8	-17.0	-16.3	-14.8	-11.7	
	Q <sub>lai</sub> (%)	7.9	8.0	4.6	3.6	2.3	3.0	4.2	3.3	10.1	8.2	24.5	27.7	21.4	
2021-2050 RCP8.5	P (%)	-3.7	-3.7	-3.7	-3.7	-3.7	-3.7	-3.7	-3.7	-3.7	-3.7	-3.7	-3.7	-3.7	
	T (°C)	1.2	1.2	1.2	1.2	1.2	1.2	1.2	1.2	1.2	1.2	1.2	1.2	1.2	
	LAI crop (%)	-15.7	-15.7										-15.7	-15.7	-15.5
	LAI pasture (%)	-7.2	-6.9	-6.7	-6.8	-6.5	-5.9	-6.6	-6.6	-7.4	-7.5	-8.1	-7.7	-7.7	
	LAI tree (%)	-4.8	-3.7	-3.1	-3.0	-2.5	-2.1	-2.7	-2.3	-3.7	-3.7	-6.6	-5.6	-5.9	
	LAI total (%)	-5.2	-4.8	-3.3	-3.2	-2.5	-2.3	-3.1	-2.4	-4.7	-4.0	-7.7	-6.9	-6.9	
	Q <sub>clim</sub> (%)	-14.6	-20.7	-13.7	-13.8	-16.3	-8.3	-14.8	-15.0	-20.1	-21.3	-23.3	-21.4	-16.1	
	Q <sub>net</sub> (%)	-13.6	-19.2	-13.2	-13.3	-15.8	-8.1	-14.3	-14.5	-18.3	-19.7	-19.0	-17.0	-13.4	
	Q <sub>lai</sub> (%)	7.4	7.8	3.8	3.8	3.2	2.5	3.5	3.4	9.8	8.1	22.6	25.9	20.1	
2071-2100 RCP4.5	P (%)	-5.0	-5.0	-5.0	-5.0	-5.0	-5.0	-5.0	-5.0	-5.0	-5.0	-5.0	-5.0	-5.0	
	T (°C)	1.6	1.6	1.6	1.6	1.6	1.6	1.6	1.6	1.6	1.6	1.6	1.6	1.6	
	LAI crop (%)	-21.1	-21.3										-20.8	-21.0	-20.7
	LAI pasture (%)	-9.8	-9.5	-9.2	-9.4	-9.0	-8.2	-9.2	-9.2	-10.2	-10.3	-11.0	-10.4	-10.5	
	LAI tree (%)	-6.6	-5.1	-4.4	-4.2	-3.5	-3.0	-3.9	-3.4	-5.3	-5.3	-9.2	-7.8	-8.2	
	LAI total (%)	-7.2	-6.7	-4.6	-4.5	-3.6	-3.3	-4.4	-3.5	-6.6	-5.7	-10.5	-9.4	-9.5	
	Q <sub>clim</sub> (%)	-19.7	-27.5	-18.6	-18.8	-22.1	-11.5	-20.3	-20.7	-26.9	-28.1	-30.1	-27.7	-21.7	
	Q <sub>net</sub> (%)	-18.3	-25.7	-17.9	-18.1	-21.6	-11.2	-19.6	-20.1	-24.7	-26.2	-25.2	-22.5	-18.6	
	Q <sub>lai</sub> (%)	7.7	7.0	3.9	3.9	2.3	2.7	3.6	3.0	8.9	7.3	19.4	23.1	16.7	
2071-2100 RCP8.5	P (%)	-5.2	-5.2	-5.2	-5.2	-5.2	-5.2	-5.2	-5.2	-5.2	-5.2	-5.2	-5.2	-5.2	
	T (°C)	2.5	2.5	2.5	2.5	2.5	2.5	2.5	2.5	2.5	2.5	2.5	2.5	2.5	
	LAI crop (%)	-28.3	-28.3										-28.5	-28.5	-28.1
	LAI pasture (%)	-13.6	-13	-12.5	-12.9	-12.2	-11.1	-12.5	-12.5	-14	-14.1	-15.4	-14.6	-14.7	
	LAI tree (%)	-9.5	-7.4	-6.3	-6.0	-5.1	-4.3	-5.5	-4.8	-7.6	-7.6	-13.2	-11.2	-11.8	
	LAI total (%)	-10.2	-9.4	-6.5	-6.5	-5.2	-4.7	-6.2	-5.0	-9.2	-8.1	-14.9	-13.3	-13.4	
	Q <sub>clim</sub> (%)	-24.0	-33.5	-23.9	-24.2	-27.4	-14.5	-25.0	-25.6	-32.0	-33.0	-35.1	-32.8	-25.3	
	Q <sub>net</sub> (%)	-22.3	-31.3	-23.0	-23.3	-26.7	-14.1	-24.0	-24.8	-29.4	-30.8	-29.2	-26.4	-21.7	
	Q <sub>lai</sub> (%)	7.6	7.0	3.9	3.9	2.6	2.8	4.2	3.2	8.8	7.1	20.2	24.2	16.6	

1017 \* P (%) is the change in mean annual precipitation in percentage, T (°C) is the change in mean annual temperature in Degree Celsius, Q<sub>clim</sub>  
 1018 indicates the climate effect on runoff, Q<sub>net</sub> is the net effect of climate and LAI on runoff and Q<sub>lai</sub> is proportion of the climate effect (Q<sub>clim</sub>)  
 1019 that is offset by the LAI effect.

1020

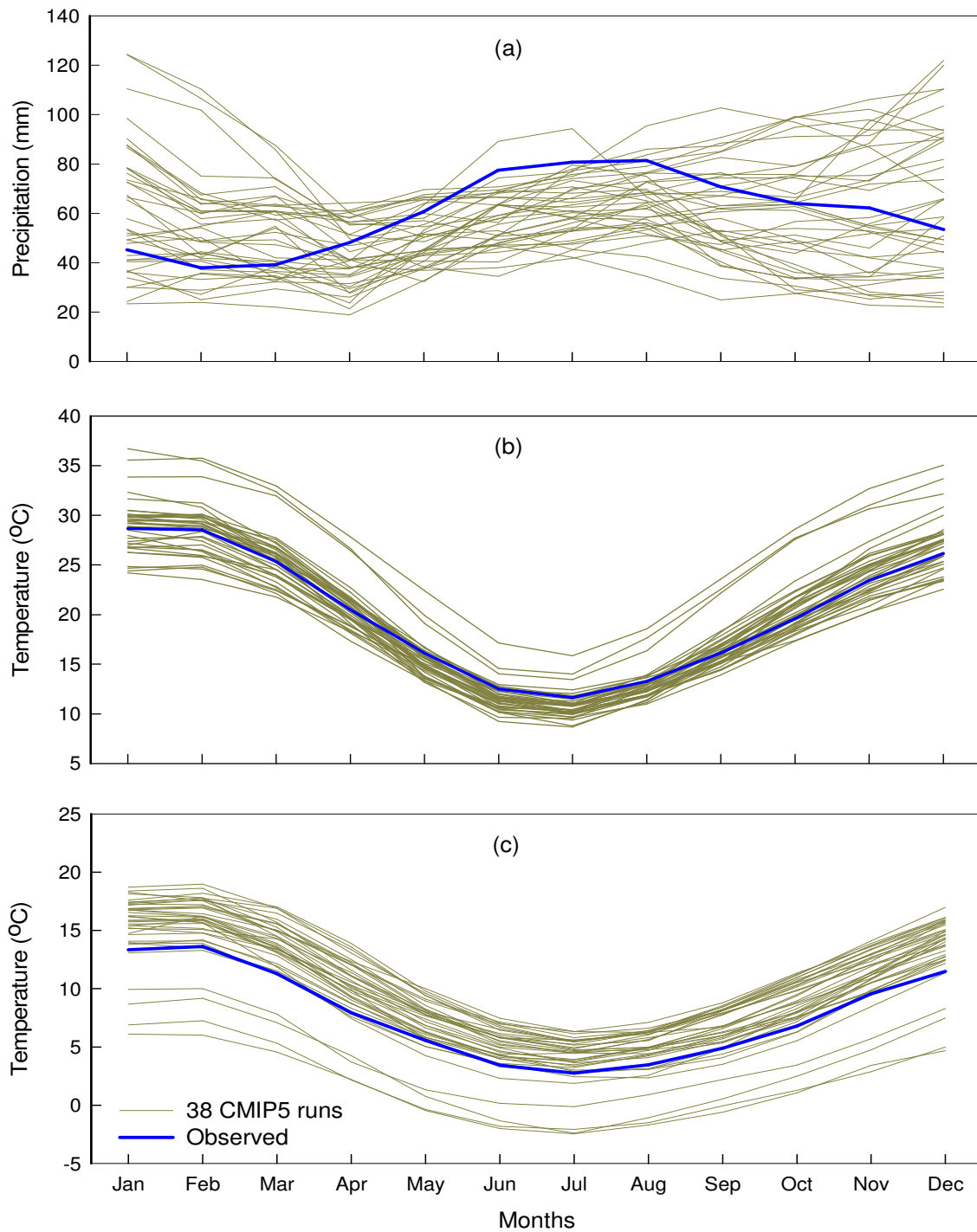
1021



1022

1023 Figure 1. Location map of the study area (a), dryness index (mean annual reference  
1024 evapotranspiration divided by mean annual precipitation) (b) and land cover type (c).

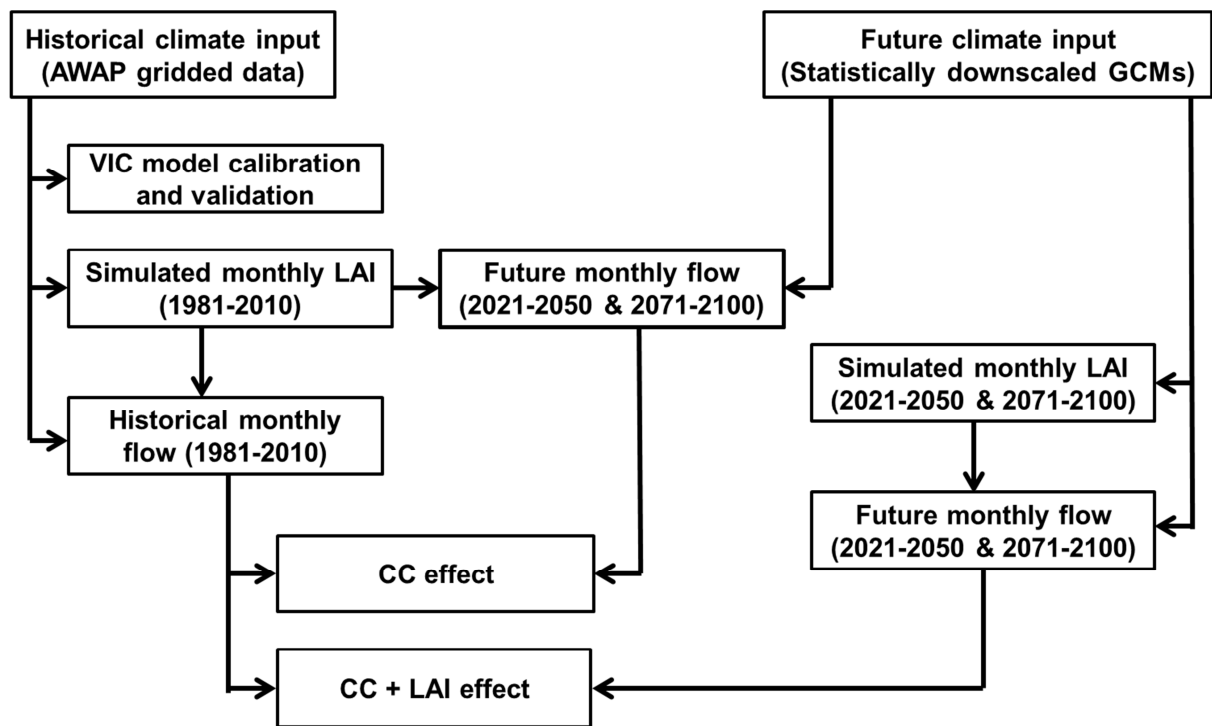
1025



1026  
 1027 Figure 2. Long-term mean monthly climate observations plotted with the 38 CMIP5 runs  
 1028 during the baseline period (1980–2010) for Goulburn-Broken Catchment (a) long-term mean  
 1029 monthly precipitation (b) long-term mean monthly maximum temperature and (c) long-term  
 1030 mean monthly minimum temperature.

1031

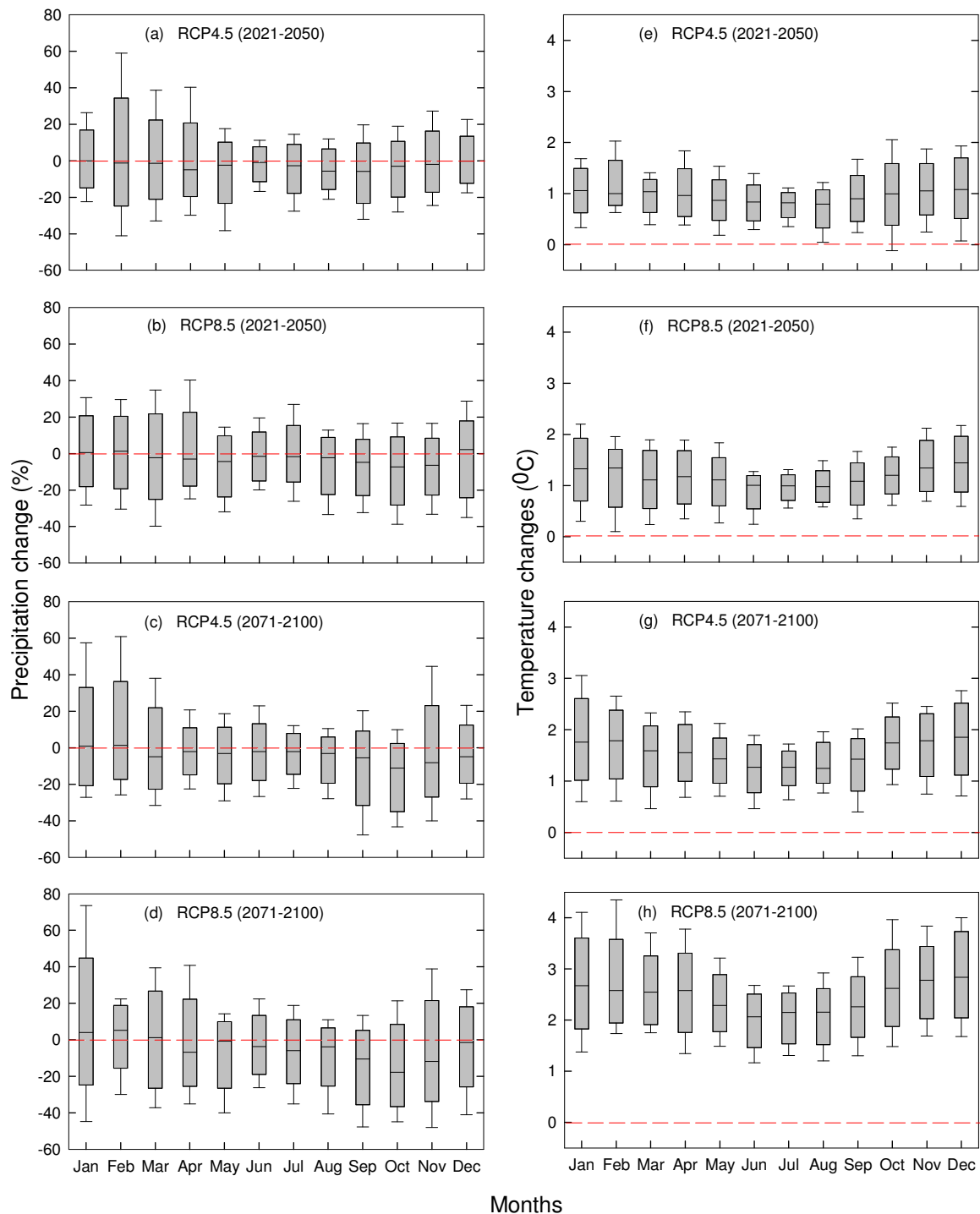




1032

1033 Figure 3. Flowchart showing the modelling experiments and calculation of effects: CC effect  
 1034 indicates the climate change effect of precipitation and temperature with unchanged LAI, CC  
 1035 + LAI effect indicates the climate change effect of precipitation, temperature and leaf area  
 1036 index.

1037



1038

1039

1040

1041

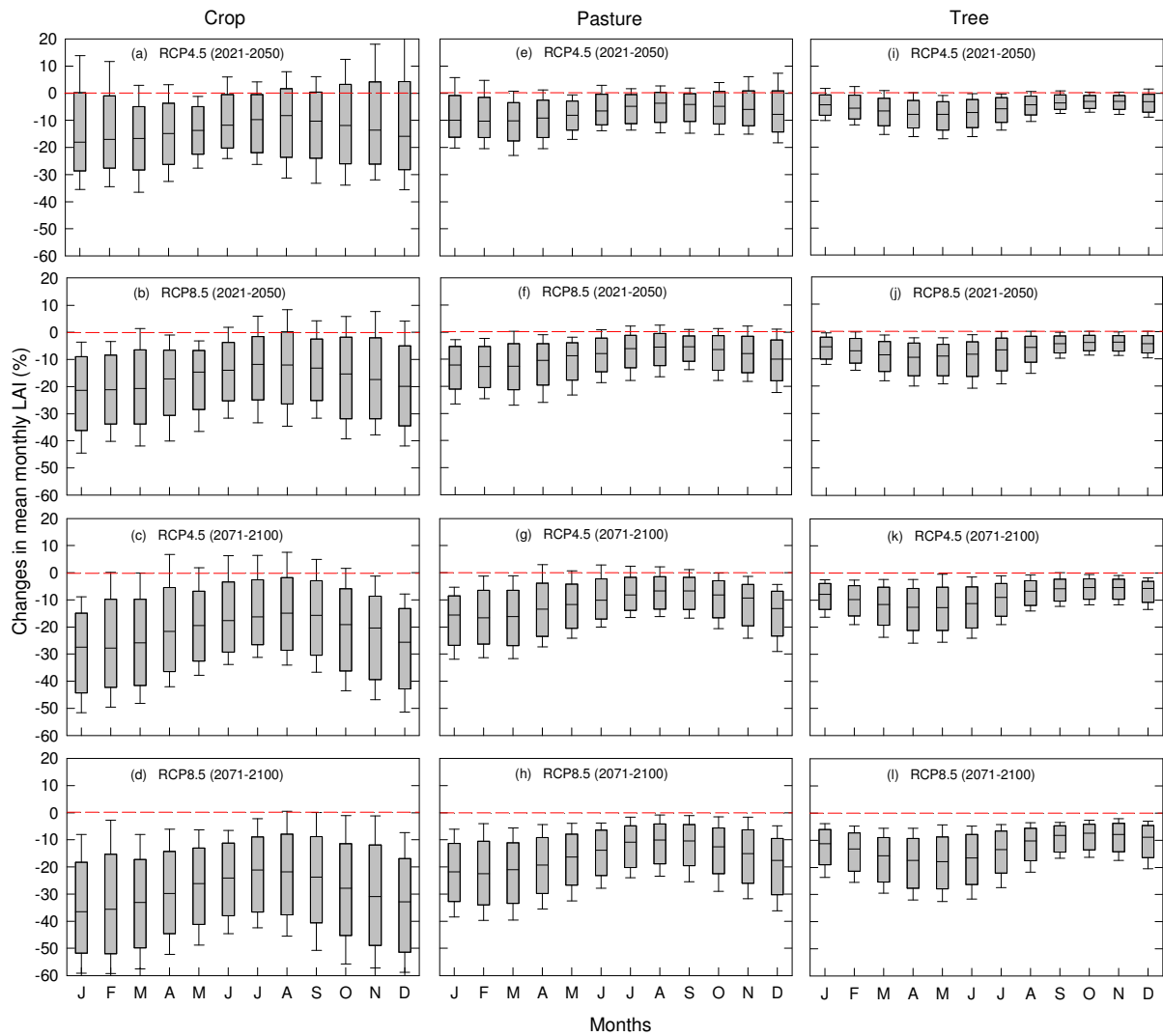
1042

1043

1044

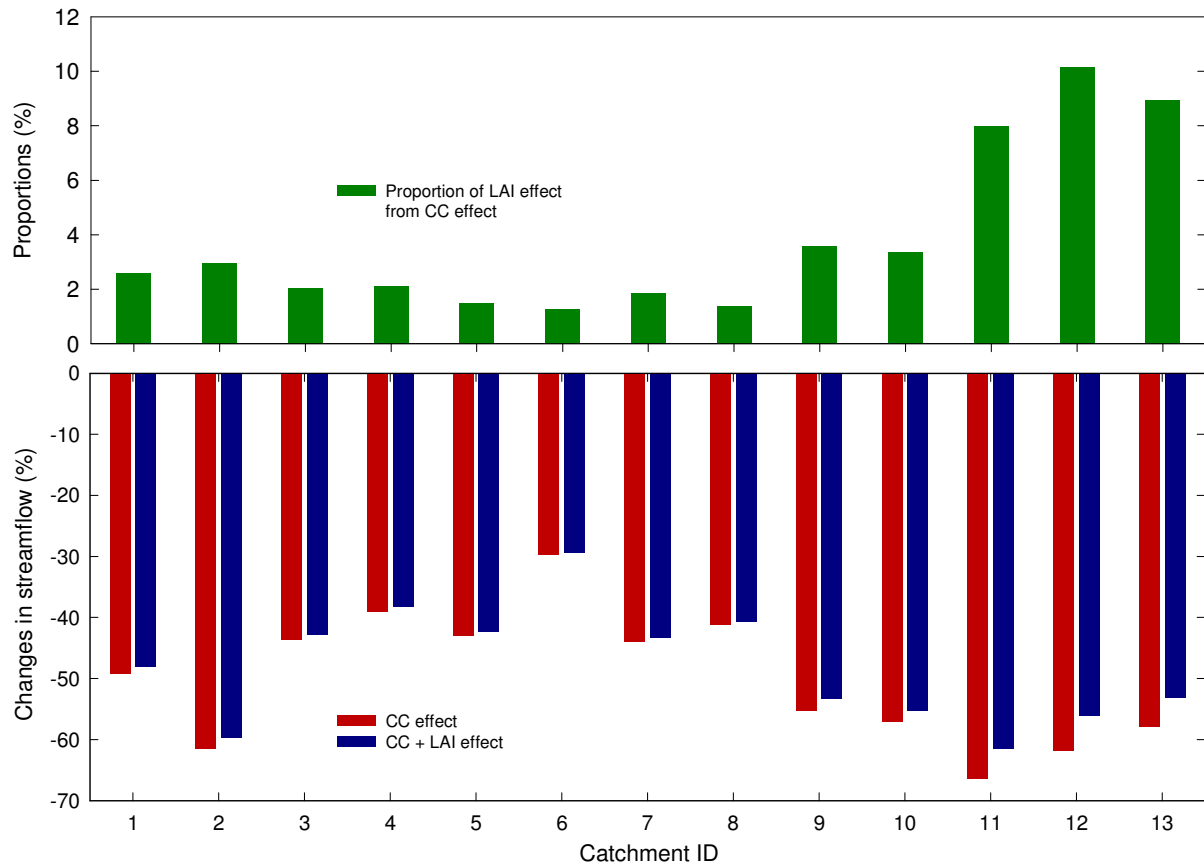
1045

Figure 4. Box plots of percentage changes in the mean monthly precipitation (a, b, c, d) and changes in mean monthly temperatures (e, f, g, h) in the Goulburn-Broken Catchment for the future periods 2021–2050 and 2071–2100 for the 38 CMIP5 runs of climate projections. Changes are relative to the historical (1981–2010) mean monthly precipitation and temperatures. The lower boundary of the box indicates the 25<sup>th</sup> percentile, a line within the box marks the median, and the upper boundary of the box indicates the 75<sup>th</sup> percentile and the whiskers are delimited by the maximum and minimum.



1046  
 1047 Figure 5. Box plots of changes in mean monthly LAI derived from the 38 CMIP5 runs for  
 1048 climate projections during 2021–2050 and 2071–2100 under RCP4.5 and RCP8.5 scenarios  
 1049 for crop (a, b, c, d); pasture (e, f, g, h) and tree (i, j, k, l) in the Goulburn-Broken Catchment.  
 1050 Changes are relative to LAI calculated using climate time series for the 1981–2010 baseline.  
 1051 The lower boundary of the box indicates the 25<sup>th</sup> percentile, a line within the box marks the  
 1052 median, and the upper boundary of the box indicates the 75<sup>th</sup> percentile and the whiskers are  
 1053 delimited by the maximum and minimum.

1054

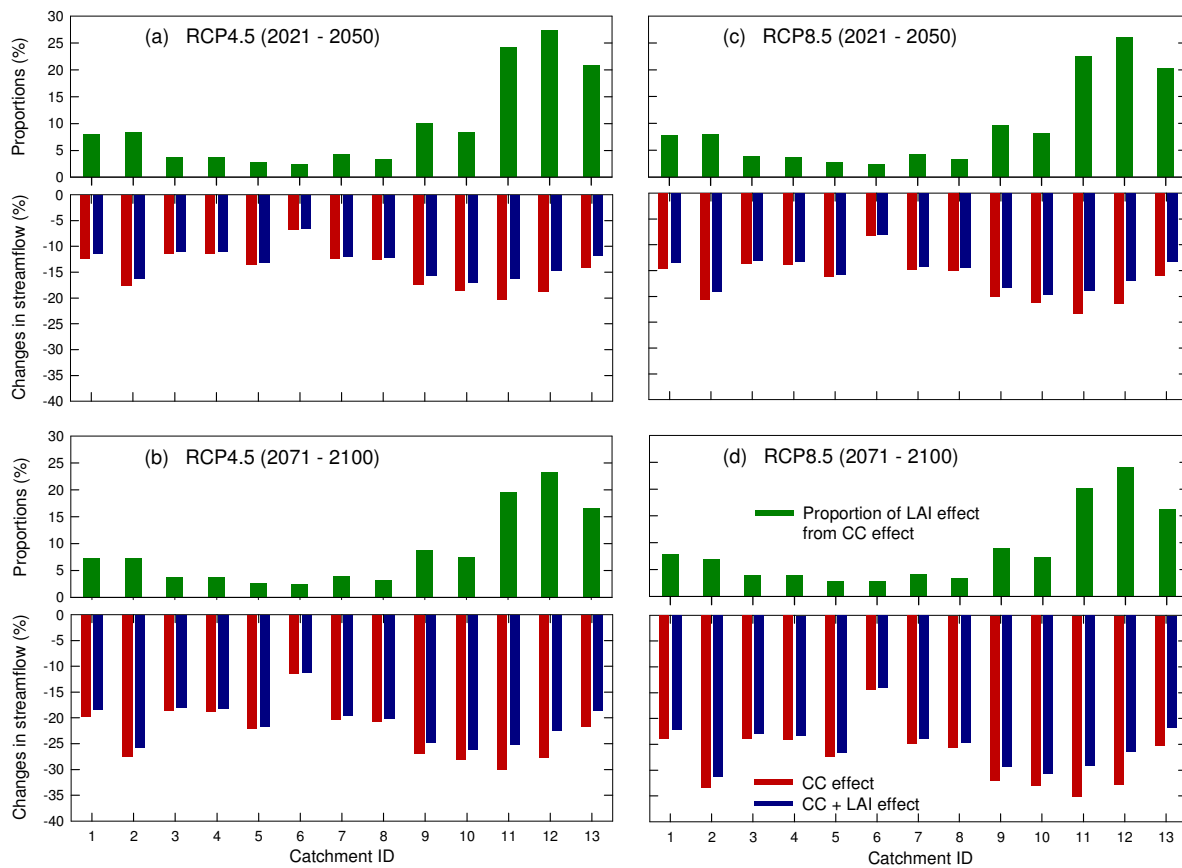


1055

1056 Figure 6. Impacts on catchment mean annual streamflow of the Millennium drought (1997–  
 1057 2009) relative to the period 1983–1995. CC effect indicates precipitation and temperature  
 1058 effect with unchanged LAI; CC + LAI effect indicates precipitation, temperature and LAI  
 1059 effect. The proportional LAI effect indicates the LAI effect as a percentage of the CC effect.

1060

1061

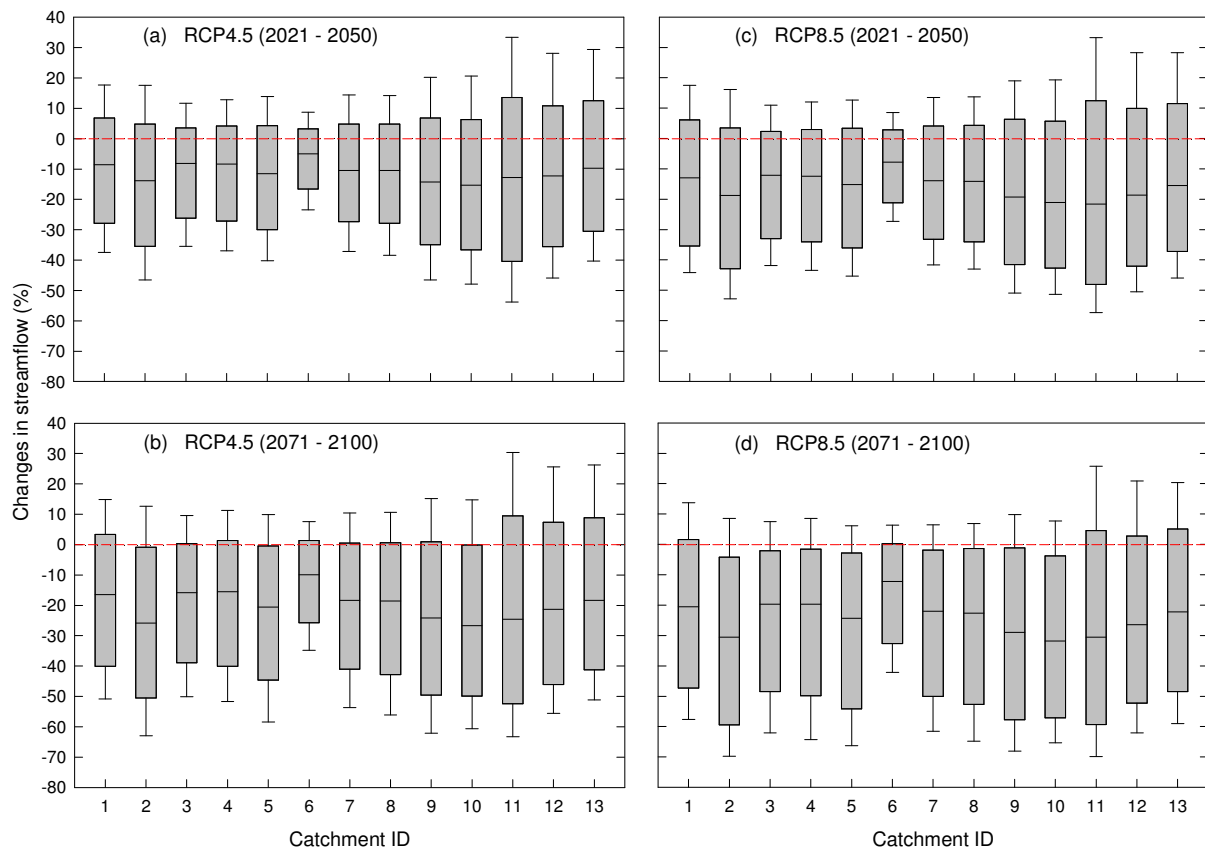


1062

1063 Figure 7. Impact on catchment mean annual streamflow average over the 38CMIP5 runs of  
1064 projected climate change for the future periods 2021–2050 and 2071–2100 under RCP4.5 (a,  
1065 b) and RCP8.5 (c, d), relative to the 1981–2010 base period. CC effect indicates precipitation  
1066 and temperature effect with unchanged LAI; CC + LAI effect indicates precipitation,  
1067 temperature and LAI effect. The proportional LAI effect indicates the LAI effect as a  
1068 percentage of the CC effect.

1069

1070



1071

1072

1073

1074

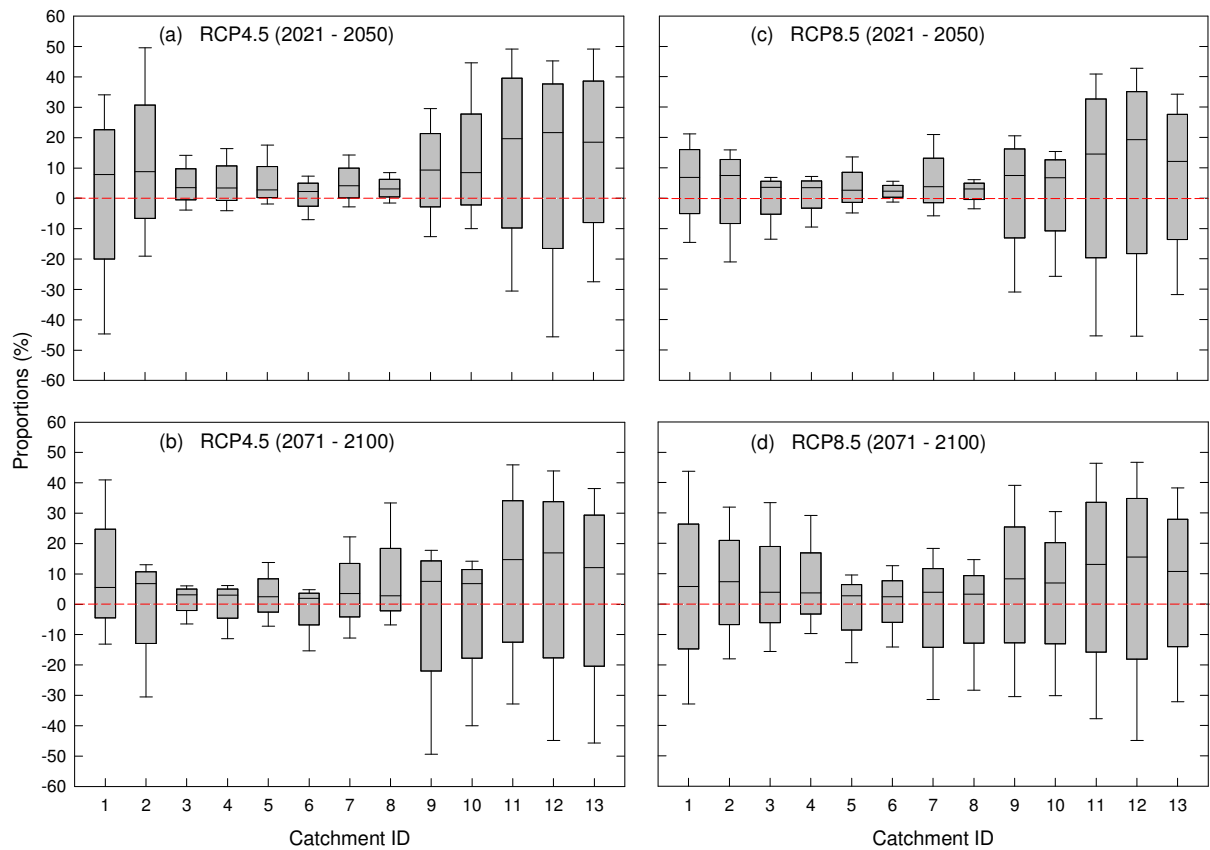
1075

1076

1077

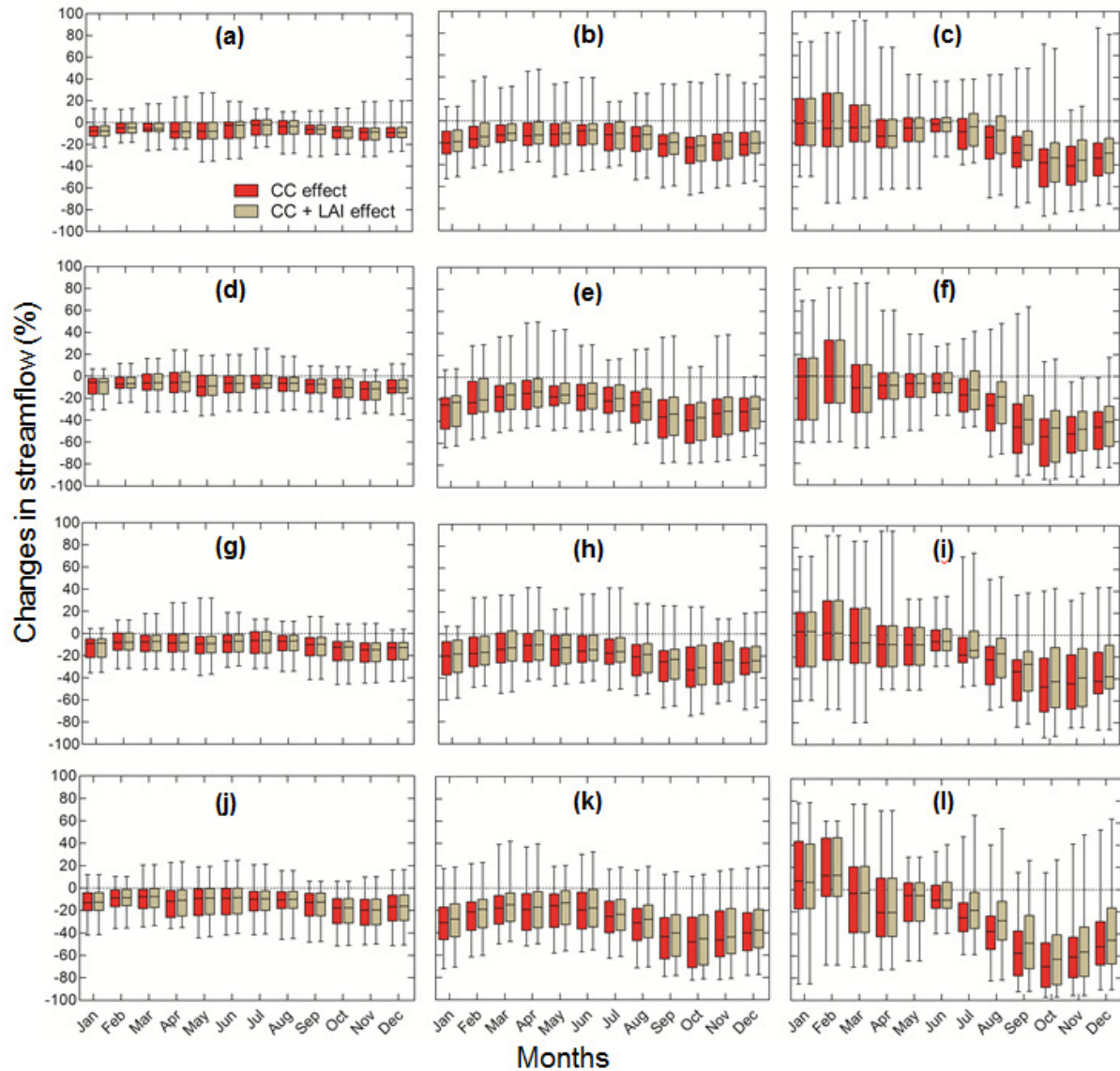
1078

Figure 8. Box plots of the net climate change (CC + LAI) effect on mean annual runoff during (2021–2050, 2071–2100) under RCP4.5 (a, b) and RCP8.5 (c, d) emission scenarios from each of the 38 CMIP5 runs. Changes are relative to the historical (1981–2010) period. The lower boundary of the box indicates the 25<sup>th</sup> percentile, a line within the box marks the median, and the upper boundary of the box indicates the 75<sup>th</sup> percentile and the whiskers are delimited by the maximum and minimum.



1079  
 1080  
 1081  
 1082  
 1083  
 1084  
 1085  
 1086  
 1087  
 1088

Figure 9. Box plots of contribution of LAI to the climate change effect on mean annual runoff for future (2021–2050, 2071–2100) climate forcing under RCP4.5 (a, b) and RCP8.5 (c, d) emission scenarios from each of the 38 CMIP5 runs as compared to the historical (1981–2010) period. The LAI effect is normalized by the effect of precipitation and temperature with unchanged LAI (i.e. CC effect) and expressed as a percentage. The lower boundary of the box indicates the 25<sup>th</sup> percentile, a line within the box marks the median, and the upper boundary of the box indicates the 75<sup>th</sup> percentile and the whiskers are delimited by the maximum and minimum.



1089

1090

1091

1092

1093

1094

1095

1096

1097

1098

Figure 10. Box plots of impacts on mean monthly streamflow from 38 CMIP5 runs of catchment 6 (a, d, g and j), catchment 10 (b, e, h and k), and catchment 11 (c, f, i and l) of projected climate change for future periods (2021–2050) and (2071–2100) under RCP4.5 and RCP8.5 respectively relative to the 1981–2010 base period. CC effect indicates precipitation and temperature effect with unchanged LAI; CC + LAI effect indicates precipitation, temperature and LAI effect. The lower boundary of the box indicates the 25<sup>th</sup> percentile, a line within the box marks the median, and the upper boundary of the box indicates the 75<sup>th</sup> percentile and the whiskers are delimited by the maximum and minimum.